ADDIS ABABA UNIVERSITY
ADDIS ABABA INSTITUTE OF TECHNOLOGY
SCHOOL OF CIVIL AND ENVIRONMENTAL ENGINEERING

SHEAR STRENGTH ANALYSIS OF RC EXTERIOR WIDE-BEAM-COLUMN JOINT

A Thesis in Structural Engineering

By: Betelhem Desalegn

February, 2024

Addis Ababa

A Thesis Submitted in Partial Fulfillment of the Requirements for the Degree of Master of Science

ADDIS ABABA UNIVERSITY

ADDIS ABABA INSTITUTE OF TECHNOLOGY SCHOOL OF

CIVIL AND ENVIRONMENTAL ENGINEERING

"Shear strength analysis of RC exterior wide-beam column joint"

By: Betelhem Desalegn

Advisor: Dr. Abrham Gebre

(May, 2024)

Approved by Board of Examiners

Dr. Abrham Gebre		June 24/2024
Advisor	Signature	Date
Dr. Bedilu Habte		June 24, 2024
Internal Examiner	Signature	Date
Dr. Edom Adane		June 25, 2024
External Examiner	Signature	Date
Dr.		
Chairman	Signature	Date

Abrham Gebre (Dr.)
Dean, School of Civil & Environmental Engineering

Declaration

I hereby declare that all information in this document has been obtained and presented in accordance with academic rules and ethical conduct. I also declare that, as required by these rules and conduct, I have fully cited and referenced all material and results that are not original to this work.

Name: Betelhem Desalegn

Signature: 

ACKNOWLEDGMENT

First, I praise and thank Almighty God and his mother Saint Mery for giving me strength and ability to start and complete this research work. Next, I'm grateful to my dear brother Solomon Desalegn whose significance in my educational journey cannot be overstated. Sol look, I put your praise next to God.

I would like to express my sincere appreciation and thanks to my advisor, Dr. Abrham Gebre, for his unwavering patience, support, guidance and understanding throughout my research work.

I would also like to extend my heartfelt thanks to my beloved family and friends, who have been blessings of Almighty God. Your support and encouragement have been a constant source of inspiration.

I would like to convey my deepest gratitude to my supportive friend Bitanya Yared and our esteemed manager, Mr. Yohannes Wale as well as all the staff members of the Lemi Kura wereda 04 building permit and control office. Your assistance and collaborative efforts have been of immeasurable value to me.

Dr. Awel Mohammed, I would like to express my gratitude for your unparalleled support while preparing this research work. Your assistance and guidance have been truly remarkable.

Lastly, I would like to thank Dr. Tesfaye Alemu and Birhanu Fekadu for their valuable assistance and support with the finite element software.

ABSTRACT

In seismically active areas where lightweight constructions are recommended, buildings with long-span floors and heavy self-weight create huge platforms. Ribbed slabs are commonly used to address this issue. Unlike conventional beams, wide beams in ribbed slab supporting frames often exceed framing column widths. Most design codes generally allow following a similar approach to the conventional beam-column joint with some additional beam width limitation which varies among those codes. Research suggests that relying solely on these limitations cannot guarantee adequate joint performance, as the seismic behavior of the joint is significantly influenced by the torsional behavior of transverse beams. This research analytically investigates the structural performance of RC wide beam-column joints with shallow transverse beams under cyclic loading. The accuracy of the FE model in predicting shear capacity performance was validated through comparison with experimental data. A parametric study using finite element analysis was conducted on 48 specimens with different LHS representative combination samples. The study primarily analyzed shear strength of the joints. Using regression analysis for specified range of values, a suggested formula considering transverse beam factors was proposed to be incorporated into the existing expected shear strength equation provided by ACI. An influential parameters of transverse beam were identified by sensitivity analysis. Concrete strength, longitudinal reinforcement ratio, stirrup yield strength, and spacing significantly affected the joint capacity. The shear capacity of the joint showed low sensitivity to changes in the yield strength of longitudinal bars. Smaller diameter bars in the transverse beam showed relatively reduced concrete damage. The study emphasized the importance of incorporating shallow RC transverse beams in the design process of wide beam-column joints. The study presents a systematic approach to improve and quantify shear capacity by considering various combinations of transverse beam parameters. The increased design options for improving shear capacity broaden the scope for practical decision-making, taking into account the availability of parameters and the ease of implementation.

***Keywords**: wide beam-column joint, transverse beam, torsion failure, shear strength*

TABLE OF CONTENTS

LIST OF FIGURES

LIST OF TABLES

SYMBOLS

f'_c	Cylindrical compressive strength of concrete
f_t	Tensile strength of concrete
f_{cd}	Design compressive strength of concrete
E_c	Modulus of elasticity of concrete
f_y	Yield strength of reinforcement
f_{yd}	Design yield strength of reinforcement
E_s	Modulus of elasticity of steel
σ_c	Concrete normal stress
ε_c	Compressive strain in the concrete
ε_{cm}	Compressive strain in the concrete at the peak stress
ε_{cu}	Ultimate compressive strain in the concrete
ε_s	Tensile strain in the steel
ε_y	Yield strain
μ_Δ	Displacement ductility factor
ζ	Potential flow eccentricity
Ψ	Dilation angle
θ	Angle in degree
K_c	Shape factor of the yield surface
ν	Poisson ratio
A_g	Gross cross sectional area
A_s	Total cross-sectional area of transverse beam bars
b_c	Width of column
b_w	Width of beam
ρ_v	Volumetric transverse reinforcement ratio
d_b	Diameter of reinforcement bar
$\frac{\sigma_{bo}}{\sigma_{co}}$	Ratio of biaxial to uniaxial compressive strength
V_j	Joint shear force

ABBREVIATIONS

ACI	American Concrete Institute
ASCE	American Society of Civil Engineers
CDP	Concrete damage plasticity
CDPM	Concrete Damage Plasticity Model
DCH	Ductility Class High
DCM	Ductility Class Medium
EN	Euro code
ES EN	Ethiopian Standard based on Euro Norms
FEM	Finite Element Method
FIP	Federation International de la Prefontaine
LHS	Latin Hypercube Sampling
LVDT	Linear Variable Differential Transformer
MRFS	Moment Resisting Frame System
NLFEA	Nonlinear Finite Element Analysis
RC	Reinforced Concrete

1. INTRODUCTION

1.1. Background

In seismically active zones, constructing buildings with long-span floors and excessive self-weight relative to the applied dead load and imposed load results in a bulky and uneconomical approach. Such massive structures become hazardous in those areas where lightweight structures are highly recommended. Using a ribbed slab is a commonly utilized appropriate solution due to its lightweight, resilience to vibration, less foundation load, flexibility in design, ability to resist cracking and cost-effectiveness for locations particularly vulnerable to seismic activity.[1, 2] Unlike conventional frame systems, ribbed slab-supporting frame connections often have beams wider than framing columns with equal shallow depth to the ribs.

Wide beam-column joints play a crucial role in ensuring the overall safety of the structure since joints must be stronger than the framing beams and columns. In addition to joint shear failure, external wide beam-column connections are susceptible to transverse beam failure in torsion. [3, 4] Although many studies have been conducted on the seismic behavior of conventional beam-column and slab-column connections, only a few studies have been dedicated to understanding the behavior of wide-beam-column joints and their application in the frames. [5]

Most current design codes, including ES-EN 2015, ACI and Euro code allow this type of joint by following a similar design approach to the conventional beam-column joint, with some additional requirements for beam width limitation that vary among those codes. [6, 7]. However, according to previous research, beam width limitations cannot guarantee adequate performance of a wide beam-column joint because such a type of joint is not only susceptible to joint shear failure but also highly vulnerable to the additional torsional effects of transverse beam. Torsion in a transverse beam is caused by the longitudinal bar of the wide beam anchored outside the column. This can produce additional joint shear stresses. [5] Hence, compared to conventional beam-column connections, wide beam-column joints have more complex load transfer and stress distribution mechanisms. Various design codes of practice specify different additional requirements for designing wide beam-column connections. Since fewer studies have been conducted to determine the effect of the transverse beam on the shear strength capacity of the joint. In this research, a parametric study have been conducted to analyze the effect of the transverse RC beam on the structural behavior of the RC wide beam-column joint subjected to cyclic loading.

1.2. Statement of the Problem

Most design codes including ACI and Euro code, generally allow reinforced concrete moment frames with wide beams in seismically active zones, following a similar approach to conventional beam-column joints with additional extra requirements for beam width limitation. However, beam width restrictions vary significantly among codes due to insufficient studies and lack of a common design approach. Previous researches have shown that beam width limitations cannot guarantee adequate performance of wide beam-column joints. These joints are susceptible not only to joint shear failure but also to the additional effects of torsion in the transverse beam and flexure around the joint. Despite these facts, new wide beam-frame buildings are designed and constructed with no particular consideration given to the torsional behavior of the transverse beams.

While numerous studies have investigated influential parameters on the shear strength of conventional exterior RC beam column joints, fewer studies have been conducted on the influential parameters of wide-beam column joints. [5] The purpose of this study is to analyze the effect of a shallow RC transverse beam on the structural behavior of RC wide beam column joints under cyclic loading using numerical analysis.

1.3. Research Questions

- Which torsional parameters of the transverse beam significantly affect the wide beam-column joint performance?
- What is the combined and separate effect of compressive strength of concrete, amount of longitudinal and transverse reinforcement ratio, yield Strength of bar and diameter of longitudinal bar of transverse beam on wide beam column joint shear strength?

1.4. Objective of the Study

1.4.1. General Objective

The objective of this research is to investigate the effect of shallow RC transverse beam on the structural performance of RC wide beam column joint numerically under cyclic loading.

1.4.2. Specific Objectives

The specific objectives of the study will be:-

I. Analytically estimate horizontal shear strength of the beam-column joint by accounting effects of torsional parameters in transverse beam
II. By using regression analysis investigating relationship between shear and those parameters
III. Performing sensitivity analysis for key parameters of the models and their distinct characteristics

1.5. Research Significance

The existing studies showed that torsional behavior of transverse beams significantly influences seismic behavior of wide beam-column connections.[8-11] In spite of this fact, torsional behavior of transverse beams are not given adequate emphasis in design and construction consideration. The majority of design codes, including ACI and EC8, do not explicitly show the contribution of transverse beams on the shear strength of this kind of joint. [2, 9] Reports indicated that the absence of torsional reinforcement in the transverse beam is a major cause of frame collapse in recent earthquakes. Therefore, it is crucial to investigate the transverse beam parameters that play a substantial role on joint strength. This will help in designing joints that can maintain the integrity and stability of moment-resisting frame structures.

1.6. Scope and Limitation of the Study

The scope of this study is focused exclusively on the analysis of exterior wide beam-column joints in reinforced concrete structures. The study does not involve experimental work but instead utilizes Abaqus general finite element software program for modeling and analyzing RC exterior wide beam-column joints. It is important to consider certain limitations of the study, such as the contribution of floor slabs to joint shear strength not being considered in the analysis and the estimation of shear strength being limited to the horizontal shear strength of the joint only. These limitations should be taken into account when interpreting the results and applying them to practical design considerations.

1.5. Thesis Organization

This thesis consists of five chapters. Chapter 1 includes the background, statement of the problem, research questions, objectives, significance of the study, and scope of the study. Chapter 2 provides a literature review of the existing research in the relevant field of this thesis. Chapter 3 explains the methodology used in this study. It discusses the experimental specimen for the validation model, the current numerical study model, its material property, test setup, and boundary conditions of the reinforced concrete wide beam-column joint sample. It also discusses finite element modeling using Abaqus software and validation of the nonlinear finite element model with experimentally tested specimens. Chapter 4 presents the analytical results and discussions of the specimens. Finally, Chapter 5 presents the conclusions drawn from the findings of this study, as well as recommendations for future work.

2. LITERATURE REVIEW

2.1. Introduction

In current seismic-resistant design for moment-resisting reinforced concrete frames, rigid connections are used to allow for ductile types of structural failure. This helps to dissipate a large amount of kinetic energy generated from lateral loads during earthquakes. Capacity design ensures that structures behave predictably under seismic loading, reducing the risk of catastrophic failure and enabling early warning before collapse.

The beam-column joint is a crucial element in transferring loads and ensuring the overall structural stability of a building. The basic design principle is that the joints must be stronger than the adjacent beams and columns, as they play a significant role in determining seismic vulnerability of the building. Even if other structural components meet the design criteria, an unsafe design of the joint region can pose a threat to the entire structure. Unlike conventional frame systems, where the width of the beam does not exceed the width of the column, in such ribbed slab supporting frame connections beams wider than framing columns are common. Most design codes generally allow RC moment frames with wide beams in seismically active areas by following a similar approach to the conventional beam-column joint with some additional requirement of beam width limitation which vary among those codes.

Researchers studied in this concern concluded that beam width limitation cannot guarantee adequate performance of the joint since wide beam-column connections, particularly exterior wide beam-column joints are not only susceptible to joint shear failure but also highly exposed to the effect of torsion in transverse beams and additional flexure around the joint which resulted from the wide beam's longitudinal bar which anchored outside the column.

This literature review covers the behavior of RC moment-resisting frame system, general concept of beam-column joints and specific wide beam column joint behavior. It also provides an overview of ACI and Euro design code specifications for such kind of joint. Additionally, the effect of transverse beams on the strength of joints with key parameters has been reviewed. Finally, the research gaps have been identified. The information has been sourced from reliable scientific journals related to the topic under consideration.

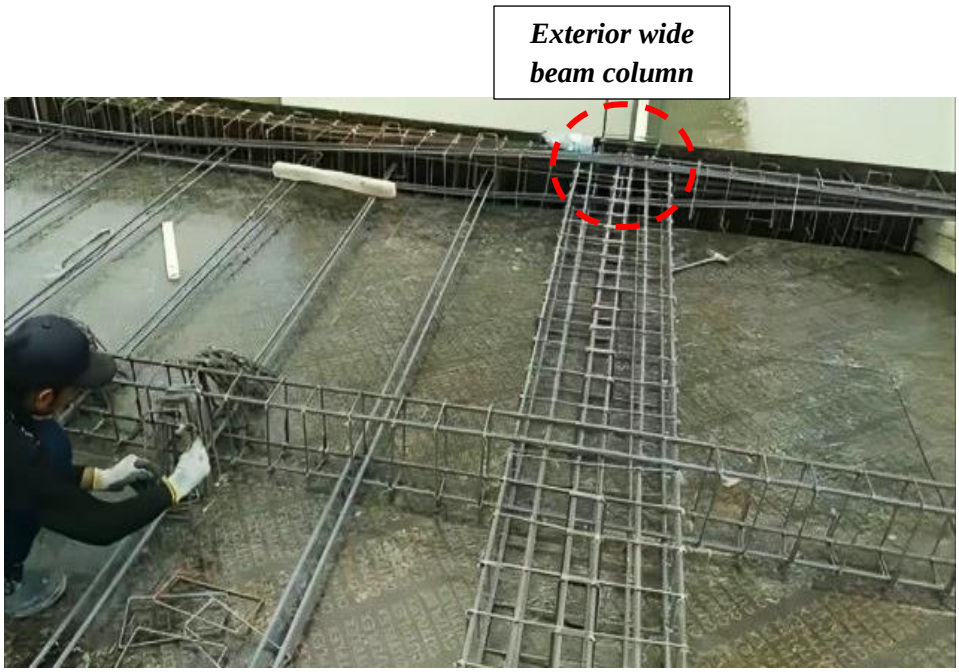

Figure 2- 1 Exterior RC wide beam column joint

2.2. RC Moment resisting frame system

A moment resisting frame system refers a structural system that can resist lateral forces such as earthquakes and wind by developing bending moments and shear forces in the beams and columns that are rigidly connected. In a RC moment resisting frame system, beams and columns are designed and detailed in a way that plastic hinges form at the ends of the beams while the columns remain elastic.[12, 13]

Frame analysis assumes that joints in a structure are strong enough to withstand forces generated from loading, such as moments, axial load, shear forces and torsion. These joints are expected to transfer these forces from one structural element to another i.e. beams to columns. However, analyzing the joints as rigid fails to consider the high shear forces that occur within a joint under seismic loading. Seismic-resistant design principles require rigid connections that enable ductile structural failures, allowing for the dissipation of a large amount of kinetic energy from lateral loads. This aligns with the concept of capacity design. The capacity design philosophy aims to ensure controlled ductile failure mechanism behavior in the structure. This involves designing the structure allowing ductile failure at a predictable location while preventing other types of failure from occurring nearby in the structure.

To emphasize the straightforward idea of capacity design, a chain with links made of both brittle and ductile materials will break when the weakest link fails. If the ductile link is the weakest, the chain will elongate significantly before breaking. If the brittle link is the weakest, the chain will break suddenly with little elongation.[14]

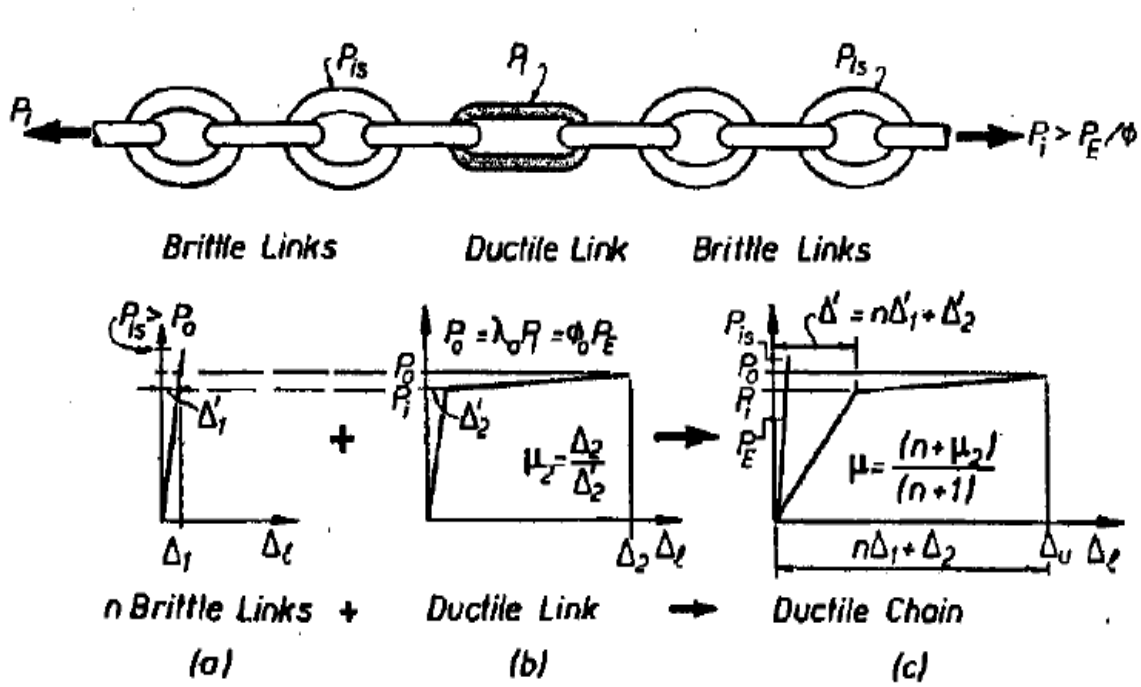

Figure 2- 2 Chain analogy concept of capacity design

The successful performance of the structure in sustaining large imposed base motions depends mainly on the energy dissipation mechanism ability of the structure to hold during the entire seismic action. [15] This can be achieved by verifying:

- The plastic hinge is carefully designed to maintain its ductility while achieving a strength level that closely matches the required level.
- The failure mode of a plastic hinge-containing member is determined by capacity development of the hinge. The failure modes are prevented by ensuring that the other modes of failure have a greater strength than the capacity of plastic hinge.
- Sections unsuitable for reliable energy dissipation are kept elastic by ensuring that their strengths exceed the requirements for plastic hinge strength.

Structures with energy dissipation require less strength, which makes them safer and more cost-effective. Utilizing ductile connections, plastic hinges in frames absorb energy transmitted by base motions, producing an efficient energy dissipation mechanism.[13, 16]

Strong Column – Weak Beam Design Concept

The strong column-weak beam design approach is a specific application of the capacity design philosophy used in structural design of frames. Providing stronger columns than beams helps to promote a beam-sway mechanism, which improves seismic performance in general by having plastic hinges develop first at the ends of beams. Since beam failure is localized, only a few parts of the structure will be affected. However, if a column fails, the entire structure may gradually collapse, which might be a catastrophic failure. Frame design primarily depends on the ductility of the beams, columns and joints that make up the frame which determines the structural ductility.[13, 16]

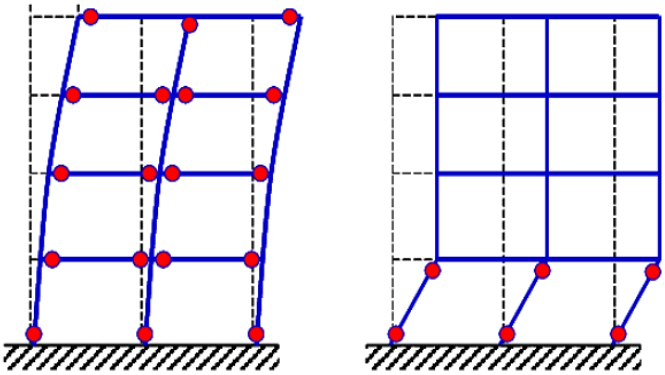

(b) Global failure mechanism

(a) Local failure mechanism

Figure 2- 3 Failure mechanisms in strong column-weak beam designs

The beam-column connection characterizes a region where the deepest part of the beam intersects with the column. Since a joint must be stronger than adjoining members, it is a critical region that needs to be designed properly to prevent brittle failure and excessive damage. The joints should have sufficient strength and confinement to transfer the forces from the beams to the columns. According to strong column–weak beam theory, column design moments at beam-column joints are calculated using actual resistant moments of the plastic hinges in the beams.

These plastic hinges occur when the beams undergo plastic deformation, typically characterized by yielding and forming a ductile region that can absorb energy. [12, 13]

As per Euro code and ES EN 1998-1:2015, the conditions are specified by equation 2.1.

$$\sum M_{Rc} \geq 1.3 \sum M_{Rb} \quad \text{..... 2.1}$$

Where: ΣM_{Rc} : sum of the design values of the moments of resistance of the columns

ΣM_{Rb}: sum of the design values of the moments of resistance of the beams framing the joint.

According to ACI 318-14 Section 18.7.3, Equation 2.2 should be satisfied in order to achieve flexural hinging in the beams rather than the columns, affecting the flexural strengths of both the beams and columns framing a joint.

$$M_r = \frac{\sum M_{n,c}}{\sum M_{n,b}} \leq 1.2 \quad \text{..... 2.2}$$

Where; $\Sigma M_{n,b}$: the sum of nominal flexural strengths of beams

$\Sigma M_{n,c}$: the sum of nominal flexural strengths of columns evaluated at the face of joint

The column flexural strength is calculated for the factored axial load consistent with the direction of the lateral forces considered which results in the lowest flexural strength.

2.3 Beam Column Joint

Beam-column joints have played an integral part in the strength and stability of reinforced concrete frame structures. The stress concentration in reinforced concrete beam-column joints is higher than that in beams and columns due to the presence of multiple load paths and the complex nature of the joint geometry. The joint is subjected to both shear and moment forces which transferred between the beam and column through the joint. [15] Due to joint discontinuity, the linear strain distribution across joints has an extensive pattern. This is among the key reasons why the joints are critical and weak zones in the moment resistance frame structures which subjected to lateral loading. [12]

2.3.1. Mechanics of joint

The transfer of forces between the beam and column through the joint in reinforced concrete beam-column joints can result in high stresses at the joint, which can lead to cracking and failure. In 1978, Paulay et al. proposed two mechanisms that govern the joint shear strength.

These mechanisms include a diagonal compressive strut and a truss mechanism.[17] The diagonal compressive strut mechanism is characterized by the formation of a diagonal strut in the joint core, which is subjected to compressive stresses. The truss mechanism, on the other hand, is characterized by the formation of a truss in the joint core which is subjected to tensile stresses.[13]

In terms of maximum shear strength and expected failure mechanism these two mechanisms govern how the joint core behaves during a seismic load. Internal forces transmitted from the adjacent framing beam and columns cause high diagonal stresses on the joint core. i.e. shear, compressive and tensile forces are applied to each joint face.[13, 18]

Figure 2- 4 **a** Illustrates that internal forces transferred from adjoining framing members to the joint core, resulting in diagonal tension and compression stresses (f_t and f_c). As a result, the joint is subjected to shear, compressive, tensile and in particular cases, torsion forces.

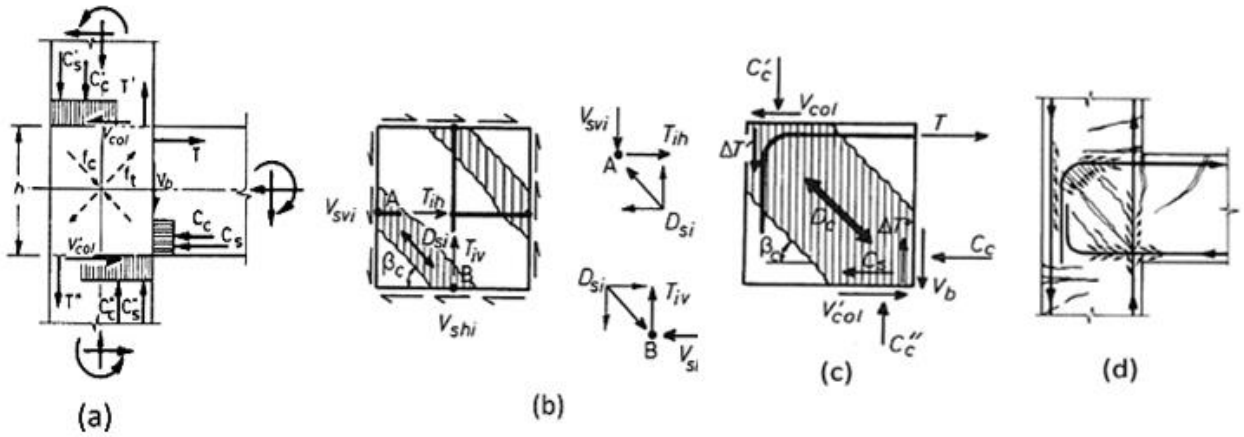

Figure 2- 4 Load transfer of RC exterior beam-column joint

The truss mechanism primarily includes the simultaneous effect of beam and column forces that are transferred to the joint core through longitudinal bars by bond stresses. Consequently, tensile resisting forces develop within the joint transverse reinforcement as shown in Figure 2-4b. [13, 18]

The joint truss mechanism cannot be developed without joint transverse reinforcement due to the limited contribution of the force transmitted by bond stresses along the longitudinal bar of the beam and column. The minor contribution reduces rapidly as bond deterioration begins inside the core. [13] The diagonal concrete strut transmits a compression force at an angle, as shown in Figure 2-4c. The concrete strut mechanism is capable of transmitting a significant amount of horizontal and vertical shear forces across the joint core. [17] The strut is anchored in a node formed inside of the standard hook of the beam longitudinal reinforcement which establishes the requirement that the hook should be bent into the joint core, as indicated in Figure 2- 4d.

2.3.2. Mode of failure

In the seismic design of new RC frames, modern seismic codes adopt a capacity design approach to ensure that a hierarchy exists between the strength of joints, columns and beams. The assessment of the performance of RC frames should therefore consider potential failures in beam-column connections. There are three common types of joint failure shown in Figure 2-5.

Joint shear failure (J-failure) occurs when the maximum shear capacity of the joint is reached without yielding beam and column (i.e. pure shear failure). This indicates that the structure will collapse before the beam and column have reached their maximum flexural capacity [19].

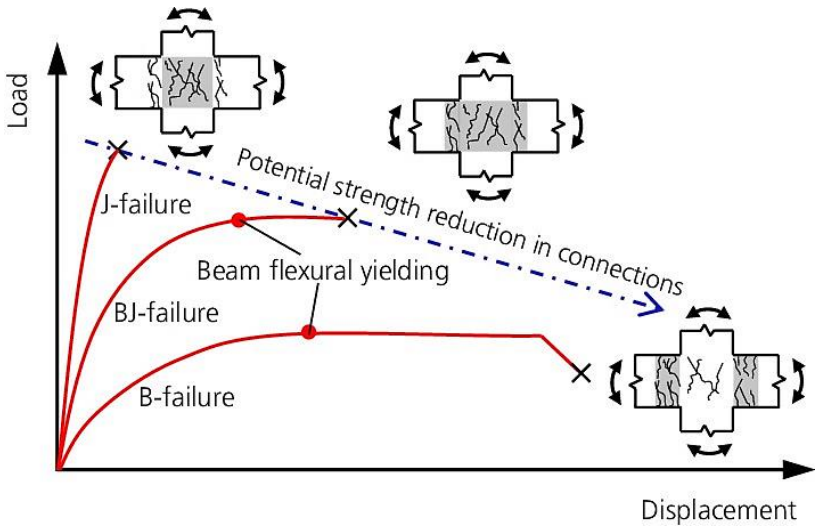

Figure 2- 5 Common type of failure on RC joint

The second type of failure mechanism is called (BJ-failure). In this type of failure, the top or bottom reinforcement of the beam yields at the face of the column shortly before the joint shear failure occurs. This type of failure is considered more ductile than pure joint shear failure [20]. The ductile failure refers the structures can endure large plastic deformations.

The failure also may occur due to the pullout of beam reinforcement from the joint core. Before reaching its joint shear capacity. This is due to the poor anchorage condition of the longitudinal beam bar. If the joint shear capacity remains greater than the demand to the end. In that case, the maximum strength may be controlled by the beam flexural capacity (B-failure) or column flexural capacity (C-failure).

2.3.3. Types of joint

In a moment-resisting frame, joints can be classified based on different relevant requirements.

2.3.3.1. Seismic loading conditions and expected deformation

Based on the loading condition of joint and expected deformations of the connected frame sections during resisting lateral loads, structural connections are divided into two categories: Type 1 and Type 2 as per ACI 352R-02.

a) Type 1 Joints: These joints embrace members that are designed to meet strength criteria with little to no inelastic deformation. These joints do not encounter earthquake loading.

b) Type 2 Joints**:** These joints have members that require deformation within the inelastic range in order to dissipate energy. These joints are subjected to seismic loading.

2.3.3.2. Location in the frame

According to their location within the frame structure and the number of beams and columns that connect at the joint interior joints, exterior joints and corner joints.

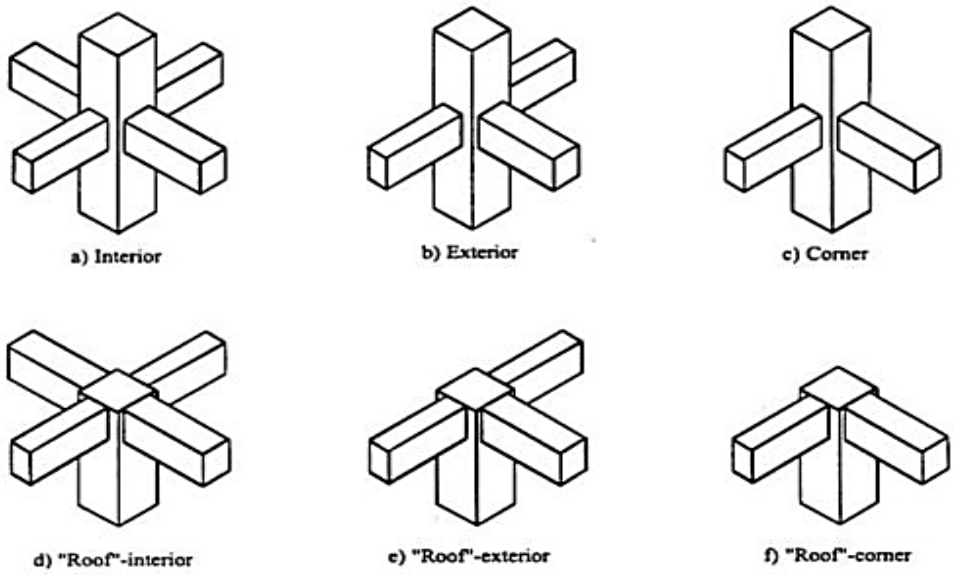

Figure 2- 6 Types of joint based on location

Geometrical dimension of adjoining members

a. **Conventional beam-column joint**: is a common type of joint where the width of the beam does not exceed the width of the adjoining column.

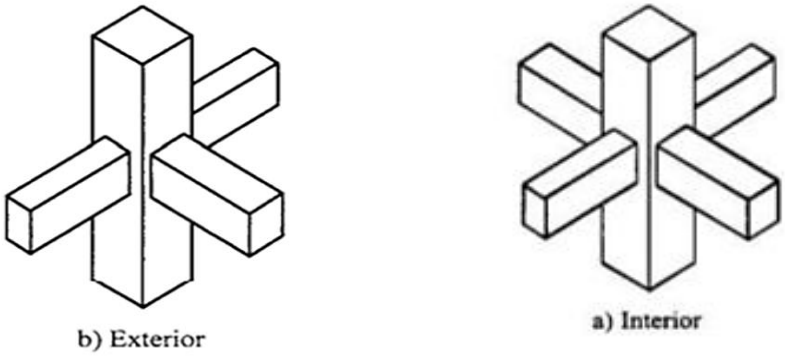

Figure 2- 7 Conventional beam column joint

b. Wide beam column joint: beams are wider than framing columns. The wide beam-column joint considered as a special case between a conventional beam slab-column connections

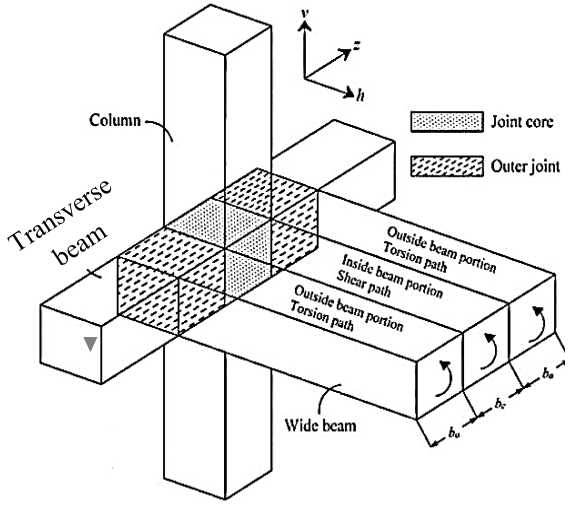

Figure 2- 8 Exterior wide beam column joint

2.4. Wide beam column joint behavior

2.4.1. Basic feature and advantages of RC wide beam-column frames

In the case of long-span floors, while heavily loaded, an ordinary frame design results in a massive platform which is hazardous in seismically active zones where lightweight construction is highly recommended. A special type of RC moment-resisting frame often constructed with wider beams joining the columns that are shallow (usually having the same depth as the slab) to support hollow slab sections. Ribbed slab supporting frame is typical example of this kind of frame.

The wide beam structural frame system provides lower self-weight as it promotes to use of hollow sections which is typically observed in ribbed slab platforms. Additionally, this frame system offers several advancements such as quicker construction, minimal resource wastage, reduced overall project costs, lower story height, optimum formwork utilization, reduced environmental pollution and improved architectural planning with better freedom of choosing column arrangement that enables more useable building space.[2, 3]

Even with its many advantages, the insufficient level of understanding about the performance of these structures causes potential benefits and applications of the wide beam system as a lateral load-resisting structure to be overlooked. To sustain lateral seismic loading safely how well the beam-column joint is designed and constructed becomes the main concern of structural designers. Researchers proposed that by improving the capacity of these connections the use of such frame systems in seismic regions can be unrestricted.[21]

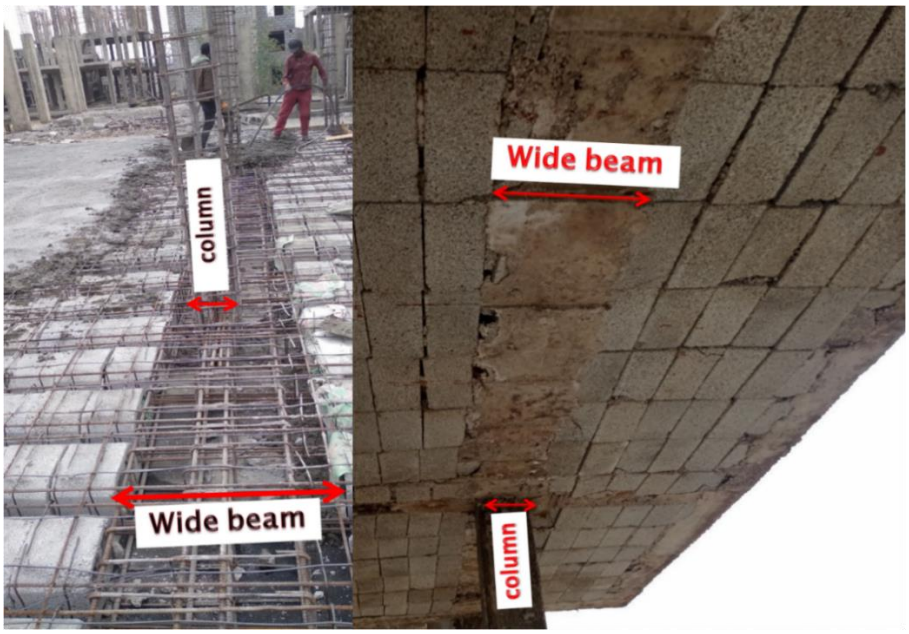

Figure 2- 9 Wide beam on ribbed slab supporting frame

Earlier research on wide beam-column connections have involved conducting experimental testing aimed at studying and optimizing the behavior of lateral sway. In order to prevent transverse beam damage from cracking by torsional moments, Russell Gentry and Wight conducted an experimental study testing 850 mm wide beam-column joints in strong seismic zones. They concluded that this could be prevented by considering the transfer of the plastic hinge bending moment to the column.[22]

2.4.2. Structural behavior of exterior wide beam-column joints

Wide beam column joint can be considered an outlier to both slab-column connections and conventional beam-column connections.

Low lateral stiffness, insufficient bending moment transmission from wide beams to the columns and limited ability to dissipate energy were observed in this type of joint resulting from insufficient understanding of structural design behavior as previously performed existing research.[21]

The exterior wide beam-column connections are extremely susceptible to transverse beam failure in torsion in addition to joint shear failure. According to test results on both the exterior and interior wide beam-column connections conducted without reinforcing on transverse beams the ductility and ultimate energy dissipation capacities of wide beam were found to be decreased significantly. Transverse beams are also exposed to experience severe torsion cracking caused by a longitudinal bar of wide beam which anchored outside of columns.[3]

There are limited specific types of research available about the behavior of wide-beam-column joints, even though numerous experimental and numerical studies have been conducted on the seismic performance of both conventional beam-column joints and slab-column joints. As a result of this, it becomes challenging to formulate general design procedure from the results of previously published research. At the Hong Kong University of Science and Technology, an extensive experimental investigation was recently carried out to gain insight in to seismic performance and failure causes of wide beam-column connections. This program has examined the effects of multiple variables, including joint shear reinforcement, beam reinforcement ratio, spandrel (transverse) beam dimension and reinforcement ratio, and beam width and column width and depth. However, testing a large number of additional specimens cannot be possible due to limitations. [3-5, 9, 10]

Finite element analysis (FEA) is a popular technique that can be utilized to accurately estimate the mechanical properties, deflections, crack pattern, and probable failure mode of RC structural members. Designing efficient material and element models in accessible finite element tool can also aid in the structural design of RC moment resisting frames with wide beam-column connections. Nevertheless, limited analytical studies on this kind of joint have been reported. Therefore, so as to ensure that wide beam structures fulfill the performance standards of practical use and to establish the basis for future study, the impacts of the previously described elements on the wide beam-column joints need to be examined.

2.4.3 Overview of prevailing design practices and codes

General Overview

According to current codes, in the design of the RC beam-column joints against the seismic load, brittle shear and bond failure should be prevented. The primary objective of these codes in the design of beam-column joints is to create plastic hinge damage in the beam region while preventing damage to the joint and column regions. Although the main suggested design methods are similar to those of conventional beam-column connections, there is additional beam width limitation requirement which vary among those codes. The restriction on beam width is the primary factor that can reduce the shear lag in the development of the full-width plastic hinge in wide beams. However, due to lack of experimental and analytical research, conclusion on this shows significant variation among codes. [6, 7]

European code (EC8, EN 1998-1)

European code (EN 1998-1) allows the use of the moment-resisting frames with wide beams in seismically active zones. According to this code to take advantage of the favorable effect of column compression on the bond of horizontal bars passing through the joint. For both ductility DCH and DCM, the beam-width limitation expressed by equation 2.3 is applicable; however, no additional specific information is offered for the design and building of wide beam–column joints as well as transverse beams.

$$b_w \leq \min [b_c + h_b; 2b_c] \quad \text{..... 2.3}$$

Where: b_w – beam width

b_c – column width

h_b – beam depth

The calculation of the shear strength of joint is determined by accounting reduction factor of compressive strength resulting from the application of tensile strain in the transverse direction and axial load ratio of the column using the equation 2.4:

$$V_j = \eta f_{cd} \sqrt{1 - \frac{\nu_d}{\eta}}\, A_j \quad \text{.....2.4}$$

Where: η – factor that accounts decrease in compressive strength of concrete resulting from the application of tensile strain in the transverse direction.

$$\eta = k\left(1 - \frac{f_c}{250}\right) \quad \text{.....2.5}$$

A_j - Effective joint area

v_d - axial load ratio of the column calculated as:

$$v_d = \frac{N_c}{A_c f_c} \quad \text{.....2.6}$$

N_c -axial load applied to the column

A_c - gross cross-sectional area of the column

American Codes (**ACI**)

The **American Codes** (ACI Committee 318) also permits the use of wide beam–column connections in earthquake-resistant frame design. It provides the largest beam width but the smallest effective joint width. Beam width is restricted as illustrated in Eq.2.7:

$$b_w \leq b_c + 1.5\, h_b, \quad \text{..... 2.7}$$

The joint shear strength calculation in the referred code mainly relies on two key factors as calculated by Eq. 2.8.: the compressive strength of concrete and the effective joint area by considering the reduction and confinement factor.

Where:

$$V_j = \lambda \phi \sqrt{f_c} A_j \quad \text{..... 2.8}$$

λ - Confinement factor

ϕ - Factor for concrete type

f_c - Concrete compressive strength

A_j - Effective joint area

2.4.4 Current researches on wide beam-column joint

Some researchers have investigated the behavior of RC external wide beam column joints experimentally. According to Lam and Teng (2003), the behavior of the joint is characterized by the interaction between the beam and the column, which can be affected by the geometry of joint and reinforcement detailing. The authors conducted experiments on twelve external wide beam column joints with different aspect ratios and reinforcement detailing. The results showed that the ultimate load capacity of joint and ductility were influenced by the reinforcement detailing, column geometry, and aspect ratio.[23]

Hatamoto et al. (1991) tested samples having beam-column width ratios b_w/b_c of 0.89, 1.77, 2.67 and 3.57 on six interior RC wide beam-column connections while the other parameters, such as the beam depth h_b and column section b_c, h_c, were held constant. According to test results, anchorage of beam reinforcement of a transverse beam should be kept to a minimum to prevent torsional failure. The beam-column width ratio should be restricted to less than 2 for the design of moment-resisting frames.[24]

As noted by Gentry and Wight (1994), column depth rather than beam depth has a greater impact on the performance of the wide beam-column connection. [25] Three exterior wide beam-column connections with transverse beams and slabs were tested by LaFave and Wight (1999). In order to examine the effects of slab participation and column aspect ratio, beam-column width ratios of 2.43-3.08 were chosen. Regarding their reaction to lateral loading, it was discovered that the wide beams performed remarkably.[26] The effective width of the wide beam in exterior joint was shown to be significantly influenced by the column depth.

Ghozali et al. (2018) investigated the behavior of two-story external wide beam-column joints using experimental and numerical methods.[27] The researcher found that the ultimate load capacity of the joint was influenced by the beam width, the column width and the beam-to-column reinforcement ratio. The numerical analysis revealed that the behavior of the joint was influenced by the interaction between the beam and the column, which affected the load distribution between them.

Zakeri and Ghannad (2015) investigated the cyclic behavior of external wide beam column joints with different beam aspect ratios using experimental and analytical methods. They found that the

behavior of joint was influenced by the beam aspect ratio, the ratio of column section, height to its width, the ratio of beam section depth to column section width and the beam-to-column reinforcement ratio. The authors suggested that the seismic behavior of joint should be evaluated considering its energy dissipation and deformation capacity.[15]

2.5. Effect of Transverse Beam

2.5.1 Transverse beam features

Transverse beams provided on the edge of each floor horizontally span the outside perimeter between two columns so as to carry the load from the slabs or walls above and transfer it to the supporting columns. These beams are often provided with narrow widths and shallow depths when employed in wide beam-column frames, as illustrated in Fig. 2-10. Despite the fact that transverse beams sustain additional load in this particular configuration, the design code does not explicitly specify the transverse beam design requirement for wide beam column joint.

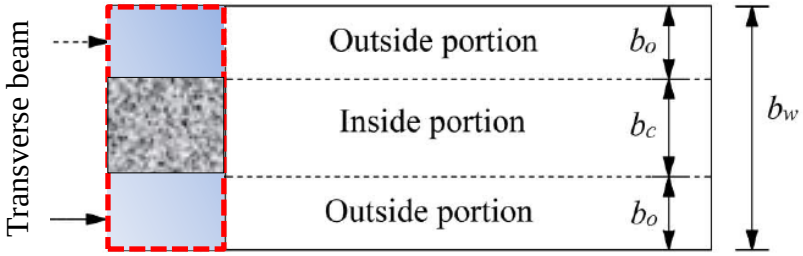

Figure 2- 10 Transverse beam on wide beam joint

Slab loads and external wall loads are transferred from floor to the outer columns by means of transverse (spandrel) beams. These beams experience simultaneous axial compression, torsion, bending moments, and shear stresses due to their interaction with the floor beams in an RC frame system, as shown in Fig. 2-11.

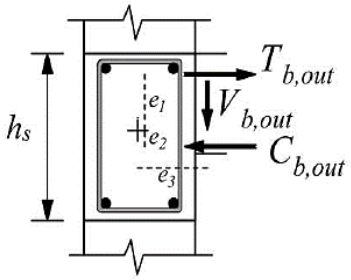

Figure 2- 11 External actions on transverse beam section

In wide beam-column frames, slab load from beams to columns can be transferred through torsion. Additionally, in wide beam frame transverse beams are also highly exposed to the effect of torsion resulting from the wide beam's longitudinal bar that anchored outside the framing column. Therefore it develops a sophisticated load distribution mechanism. While designing a transverse beam, it is important to give greater emphasis on addressing torsional behavior.[5]

2.5.1.1. Torsion

Torsion develops when loads are applied in both horizontal and vertical axes, resulting in moments that do not pass through the shear center of the beam. The total torques (shear force times distance from the shear center) acting at a given section determines the produced torsion to the beam at that cross-section can be calculated by Eq.2.9.

$$T_u \le \phi\left(1.41\sqrt{f_c'}\frac{A_{oh}^2}{p_h}\right) \le \phi T_n \quad \text{.....2.9}$$

Where: $T_u = 1.25\ T_s$

T_s = Torsion in the beam

ϕ = Strength reduction factor

T_n = Nominal torsional moment strength

A_{oh} and p_h represent the area bounded by the centerline of the innermost closed transverse torsional reinforcement and the perimeter formed by the centerline of the outermost closed transverse torsional reinforcement respectively.

2.5.1.2. Torsion Type

Two distinct torsion types in reinforced concrete structures are identified based on their structural response under torsional loading.

I. Compatibility Torsion

This kind of torsion is caused in a member by rotations (twists) applied at one or more locations along the span of member. The torsional stiffness of the section influences the resulting twisting moments. Since these moments are typically statically indeterminate as shown in Fig.2-12, the floor beam system's (rotational) compatibility is required for their analysis. This situation arises when the member's compatibility of deformation remains unchanged and the torsional moment can be decreased through the redistribution of internal forces.

In the analysis of a structure, the torsional resistance or stiffness of members has not been considered, and no special torsion calculations will be required. Another name for this kind of twisting is secondary torsion.

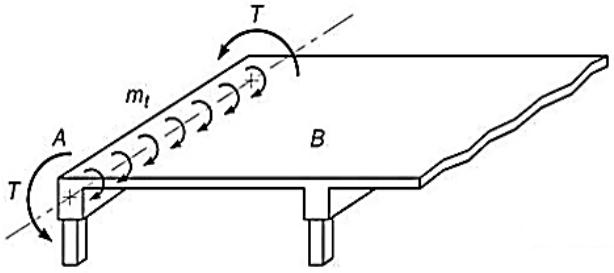

Figure 2- 12 Compatibility Torsion

II. Equilibrium Torsion

When the member can only sustain the action of an external load by producing a torsional moment, this refers to equilibrium torsion and is frequently found in statically determinate structures. The development and magnitude of twisting moments in a structural member being independent of the member's torsional stiffness to conserve static equilibrium with external loads is related to this.

This kind of torsion has to be taken into account in design. It is calculated by statics analysis. The full torsion that the member transfers to the supports must be addressed in the design of members. Furthermore, the ends of member must be properly constrained so as to enable the member to successfully withstand the induced torsion. In general, the eccentricity in the loading (regarding the shear center of cross-section) causes equilibrium torsion in beams supporting transverse overhanging projections as shown in Figure 2-13

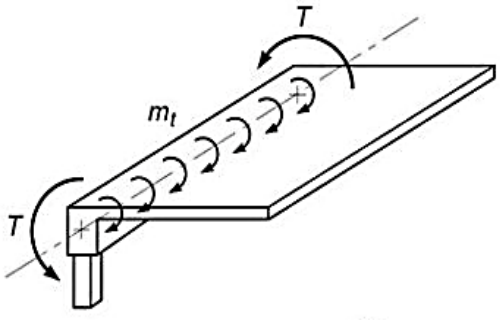

Figure 2- 13 Equilibrium Torsion

2.5.2. Researches on the transverse beam related to wide beam column joint

A study conducted at Hong Kong University of Science and Technology by S.H. LUK and J.S. KUANG investigated the seismic behavior of reinforced concrete exterior wide beam-column connections. Using ABAQUS computational simulations, this study compared the seismic behavior of wide beam-column connections and conventional beam-column connections. The results indicate that wide beam-column connections with adequate reinforcement exhibit enhanced deformability and load transfer, leading to reduced pinching. Moreover, the joint shear stress is higher in wide beam-column connections due to fewer diagonal cracks and the confinement provided by transverse beams. The orientations of concrete diagonal struts within the joint core and transverse beams vary depending on the beam width, affecting the development of the strut-and-tie model. Overall, the research emphasizes the significance of reinforcement design and load transfer paths in wide beam-column connections to enhance their seismic performance.[21]

Behnam, Kuang, Wong, Huang and Al-Mahaidi derived an analytically based beam-width limitation for RC wide beam–column connections for the design of wide beam moment-resisting frames. The concept of effective beam-width is discussed. The torsion caused by transverse beams and the flexure associated with the joint are taken into account in the suggested effective beam width model. The un-cracked stiffness of wide beam and transverse beam are used in the suggested approach. Torsional cracking of transverse beams should be eliminated by proper design so as to minimize substantial reductions of stiffness and strength.[5]

A series of experiments were conducted on two full-scale exterior wide beam-column connections by H. Behnam, J. S. Kuang, and K. Abdouka. Excluding the reinforcement detail in the transverse beam, the specimens have the same dimensions and reinforcement detailing. While the other specimen had no reinforcement in the transverse beam, the control specimen included both longitudinal and transverse reinforcement. The findings of the test show that the control specimen's failure mode was ductile with beam flexural hinging followed by joint and transverse beam torsional failure, whereas the failure mode changed to brittle torsional failure of transverse beam in the other specimen.

The publication of A. Benavent-Climent presents an experimental evaluation of the seismic behavior of RC wide beam-column connections that are primarily intended for gravity loads. A two-thirds scale model with one exterior and one interior connection is established, and then on a shaking table, it is subjected to seismic simulations until it collapses. According to the test results, (a) the drift at yield is three to six times greater than, for instance, the 0.5% allowed by Eurocode 8 in order to meet the "damage limitation requirement;" (b) There is no failure of the beam-column connections; (c) The torsion of the spandrel beams determines the maximum strength and affects a complete load-displacement relationship of the external connections. A nonlinear model for estimating the hysteretic behavior and the connections' failure is developed based on the test findings.[28]

J. S. Kuang and Hamdolah Behnam's paper on April 11, 2017 states that wide-beam reinforced concrete floor is commonly recognized as one of the most effective beam-and-slab floor systems in buildings. However, because of an absence of information regarding the seismic behavior of wide beam–column connections, the system's potential benefits as a lateral load-resisting structure are frequently underestimated. Design codes impose restrictions on beam width in order to minimize the impact of shear lag on the design of full-width plastic hinges and to attain the predicted capacity. Unfortunately, various design codes have adopted empirical design formulas for the beam width limitation, with remarkably varied outcomes, due to a lack of significant experimental and analytical investigations. Based on test findings that are currently accessible, parametric studies of the influence of important parameters on the behavior of wide beam–column connections are carried out in this study. Torsion of transverse beams and flexure around the joint center are taken into account in the analytical development of an effective beam-width model through the use of the equivalent-frame representation.[10]

The CDP model was validated by Hamdolah Behnam, J.S. Kuang and Bijan Samali through an evaluation of the experimental outcomes of four full-scale, external wide beam-column connections with the results of the finite element analysis (FEA). Additionally, they examined the FEA results' sensitivity to various model parameters and discussed about their essential characteristics.[10] In terms of the load-displacement response, crack patterns, reinforcement yielding, and failure mechanisms, the FEA results and the testing results coincided closely.

The strength, stiffness, ductility, and energy dissipation of the connections have been demonstrated to be significantly influenced by the column axial load, column and beam dimensions, beam bar anchorage ratio, and spandrel beam reinforcement, according to the parametric study. For estimating the behavior of RC wide beam-column connections, the CDP model proved to be reliable and effective tool. The parametric study offered helpful information for developing and accessing such types of joint.

2.5.3. Current researches on torsional capacity of RC beams

Haroon et al. (2021) developed an Artificial Neural Network (ANN) model using 159 RC beams with various shapes, reinforcement ratios, and loading conditions. The model predicted ultimate torque and angle of twist, with concrete area and reinforcement factor having the most significant influence. These authors also studied the effects of different parameters on the torsional behavior of RC beams using parametric analysis. [29] Initially, neither the enclosed section size effect nor the cross-sectional dimension effect was detected. The variables related to concrete size did not yield any noticeable variation in the torsional strength of the reinforced concrete beams. Second, the torsional strength of the concrete, which peaked at 90 MPa, showed a positive correlation with its compressive strength. Third, the amount of longitudinal reinforcement had an excellent impact on the torsional strength. Lastly, comparable patterns were found for the effective quantity and less-effective yield strength of the transverse reinforcement-related variables. With increasing spacing, a reduction in torsional strength was observed.

Mohammad Rashidi conducted experiments on 12 concrete beams with different types of stirrups and longitudinal reinforcement under pure torsion so as to investigate the effect of reinforcement type on torsion strength of concrete beams. It was found that as the percentage of reinforcement increases, the ductility factor rises as well. Comparing the sample with transverse and longitudinal bars to the sample without reinforcement, the torsional strength and ductility of the former have risen by 95% and 50%, respectively. Compared to longitudinal bars, transverse bars are of greater importance in determining the torsional strength of reinforced concrete beams. It is remarkable that the torsional strength of reinforced concrete beams cannot be enhanced just by transverse or longitudinal bars, and that both of these elements are necessary for the beams to exhibit favorable torsional behavior.[30]

In 2020**,** Ibrahim, M.S., Gebreyouhannes, E., Muhdin, A., and Gebre, A. conducted a study to analyze the effect of concrete cover thickness on the torsional behavior of reinforced concrete (RC) members.The investigation involved nine RC beams with varying clear concrete cover thicknesses, ranging from 16 mm to 46 mm. These beams were subjected to experimental testing under pure torsion. The experimental results revealed that the thickness of the cover concrete has a significant effect on both the pre-peak and post-peak torsional behavior of RC members. Additionally, the study examined the predictions made by commonly used codes such as ACI, CSA, and Eurocode. It was found that ACI tends to provide highly conservative estimates, particularly as the cover depth increases. The study also investigated the influence of transverse reinforcement spacing and compressive strength of the concrete.[31]

Study of A. Prabaghar and G. Kumaran compares the experimental findings with the theoretical torque-twist curves for a range of cases. The effect of different variables on the torsional behavior of GFRP reinforced beams is also covered in this research including the transverse stirrup spacing, the ratio of longitudinal reinforcement in the beam, and the concrete grade. The ultimate torque is calculated using the space truss analogy and the softened truss model. It is observed that the grade of the concrete and the percentage of longitudinal and transverse reinforcements improve with the torsional strength and twist angle.[32]

2.6. Research gap

Examining the literature on the behavior of exterior wide beam-column joints exposes two important traits. First, in addition to joint shear failure, exterior wide beam-column connections are particularly vulnerable to transverse beam torsional failure. Second, the torsional behavior of transverse beams has a major effect on the overall seismic behavior of large beam-column connections. .

The research gap in this study is evident in the limited attention that has been given to the effect of the transverse beam on the seismic performance of exterior wide beam-column connections. While previous investigations have explored the effects of transverse beams on seismic behavior in conventional beam-column joints and slab-column joints, the role of the transverse beam in the exterior wide beam-column joint of buildings has received little emphasis.

3. Methodology

3.1.General

The finite element method is mostly used to simulate the linear and nonlinear analysis of different structures. The experimental tests require more time and cost. The 3D finite element analysis has been developed to investigate the effect of specified parameters of transverse beam in shear strength of wide beam column joint. The numerical modeling specimens were carried out using a computer program based on the nonlinear finite element technique; ABAQUS/CAE software program (Simulia, 2022). In general, this specific chapter First, a description of the model specimens with details of shape and reinforcement is provided, after that, the necessary input modeling for nonlinear finite element analysis is illustrated. The RC wide beam column joint under combined axial and cyclic loads is simulated using material property models, element type, meshing, boundary conditions, loading and solution methods. Lastly, FE analysis validation with an acceptable fit between the numerical and experimental result will be presented. The cyclic load hysteresis with their envelope curve, maximum lateral load results, and concrete damages are the results that were used to validate the experimental result.

3.2. Description of the Experimental model for Verification Analysis

The validation of finite element analysis is done based on previous experimental work of Behnam & Kuang, (2018) since numerical model is regarded as valid while its simulation agrees with the verification of the experimental data. The geometrical characteristics of the model were kept in the numerical investigation according to the test specimens. For concrete, eight-node hexahedral (brick) elements (C3D8R) were used. The reinforcements were modeled using two-node linear truss elements (T3D2). The reinforcement and concrete were bonded using the embedded method, which ensures a perfect bond and displacement continuity between the steel and concrete. By applying the tension stiffening in the concrete model, the interaction between the concrete and reinforcement after it cracks, such as bond slip and dowel action, has been incorporated. The boundary conditions were applied to the reference points of the column end surfaces using the coupling constraint, following the same test setup. A lateral displacement was imposed in the beam end after the axial load on the column was applied in two stages.

3.2.1. A geometric model for experimental test

The beam and columns are terminated at mid-span and mid-height, respectively, where inflection points are expected to occur under lateral load, for sample that represent a section of the framing system. All specimens of the columns had a height of 3100 mm and uniform cross sectional dimensions of 300 * 360 mm. The beams measured 1500 mm in length and 300 mm in depth. Specifically, the beam width ratio for specimen S4 was 2.5. The transverse beam with a cross-section of 360 mm by 300 mm was located across the wide beam specimens, having a shallow depth. The samples had a wide beam width of 750 mm.

Transverse beams in the samples consisted of eight D16 longitudinal bars with a D10 closed stirrup placed at a center-to-center spacing of 70 mm. The test setup, loading, and damage at 4% drift ratio are shown in Fig.3-1.

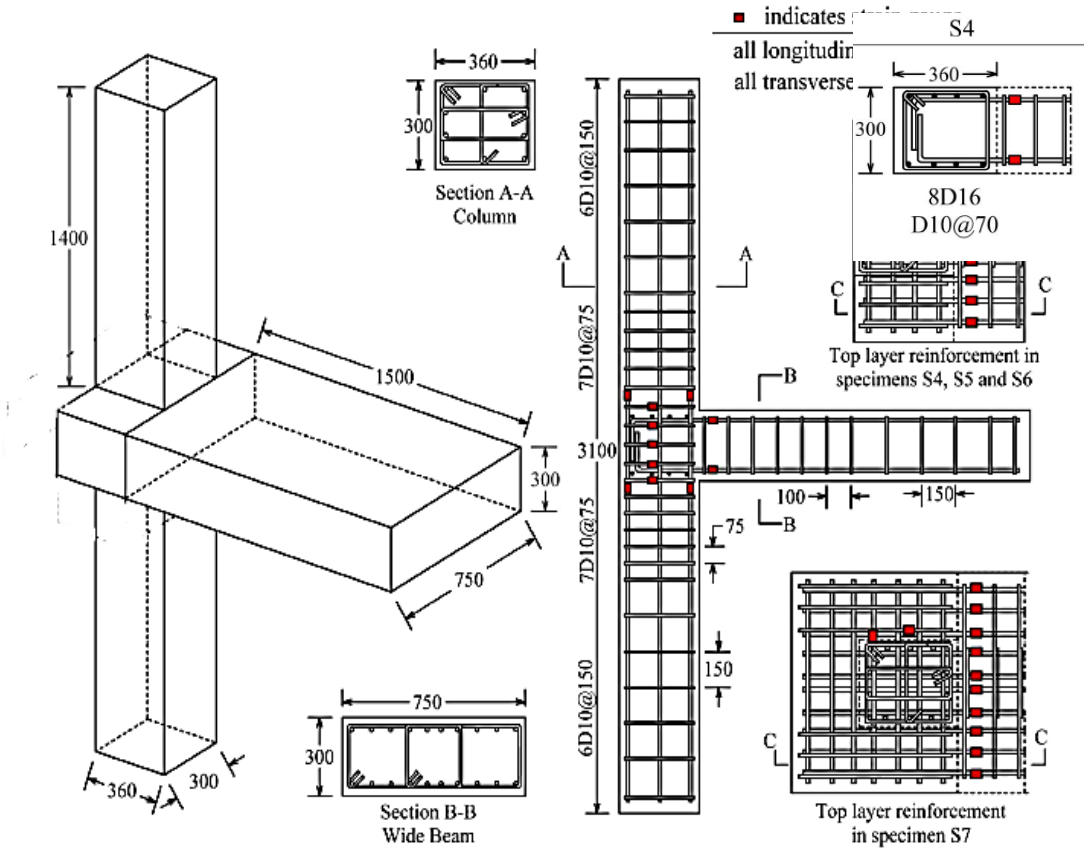

Figure 3- 1 Geometry and Reinforcement detailing of the sample model (S4)

3.2.2. Material properties for experimental test

3.2.2.1. Concrete

Table 3-1 Concrete properties of specimen

Specimen	f'_c MPa	E_c[a] MPa	ε_0 (%)	ε_u (%)	f_t[b] MPa	G_f N/mm	Poisson's ratio (ν)	Density tonne/mm^3
S4	34.7	27,685	0.250	3.5	2.80	0.083	0.2	2.4E-009

[a] $E_c = 4700\sqrt{f_c}$

[b] Measured using four point loading tests on test day

3.2.2.2. Reinforcement bar

Table 3-2 Reinforcement properties of specimen

Reinforcement	S4	
Bar diameter (mm)	10	16
Yield strength f_y (MPa)	511	558
Ultimate strength f_u (MPa)	620	642
Yield strain (%)	0.255	0.279
Ultimate strain (%)	12	9

3.2.3. Test Setup, Loading and Boundary Conditions of Experiment

The original configuration of each beam-column assembly was rotated by 90 degrees in which the column was horizontal and the beam was vertical as shown in Fig.3-2.

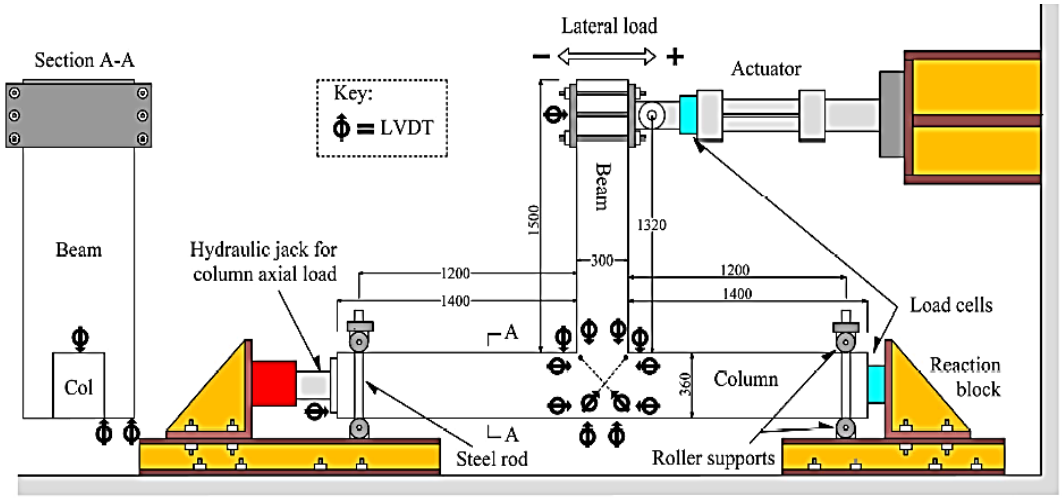

Figure 3- 2 Simplified representation of the experimental setup

The beam tip and the left and right sides of the column were all pin-connected to represent the state of the inflection points of a bending moment diagram of the frame under lateral loading (zero bending moment). Steel rods were used to link the front roller supports to the rear of the column at each end as shown in Figure 3-2. As a result, the column was able to rotate at its ends under a flexural bending moment and move laterally in the direction of an axial force, but it was fixed vertically.

The column was initially subjected to an axial compressive force of 480 kN using a hydraulic jack at one end, with the load cell placed at the reverse end controlling the axial load. Throughout the test, a constant axial load was delivered in a force-controlled mode. Then, using a horizontal actuator, the lateral reversed cyclic displacement (Δ) was introduced to the top of the beam. The utilized lateral load technique was selected in accordance with the ACI 374.1-05 (ACI 2005) acceptance requirements.

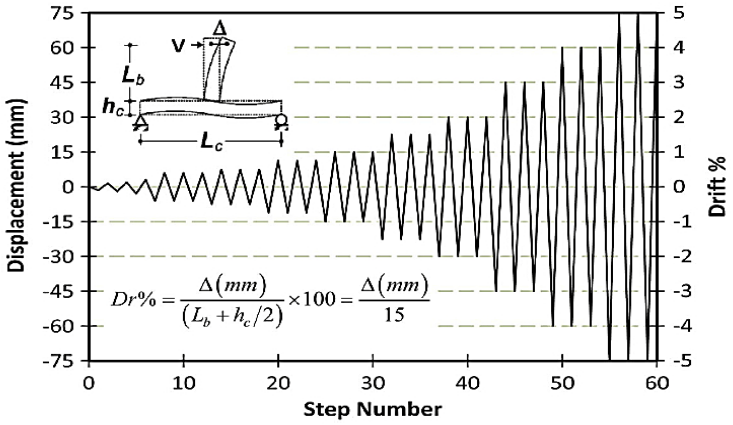

Figure 3- 3 Cyclic displacement applied during the experimental test

In order to assess the strain levels that formed at different loading steps, specimens were carefully instrumented by attaching strain gauges at key points found on the reinforcement bars. Additionally, to record the displacement, linear variable displacement transducers were placed at various points on the specimen.

3.3. Numerical Investigation

3.3.1. Finite element method analysis

Finite element modeling is a very useful tool for effectively analyzing the behavior of reinforced concrete structures that are challenging to analyze through experiment, including joints under various loading scenarios such as static, dynamic, cyclic, seismic, thermal, and blast and boundary conditions. FEM can offer a number of advantages, including as accuracy, efficacy, versatility, simplicity of use, illustration, and verification.

Abaqus is one of the Finite Element Analysis (FEA) software packages that have many products designed to meet multiple applications. Geometry, boundary conditions, element types, material properties, and the nonlinear analysis solution are defined during the pre-processing step. Visualizations of the results are created during the post-processing stage. FE modeling techniques were applied to simulate the RC wide beam column joint with different parameters. The procedure incorporates specification of geometry, material property, meshing, interaction, loading, boundary conditions, and analysis.

3.3.2. Geometrical modeling

The control specimen was modeled in ABAQUS as defined by Behnam & Kuang, (2018) experimental detail. The columns had heights of 3100mm and cross-sectional dimensions of 300*360mm. The beams were 1500mm long and 300mm deep. The samples wide beam had a 2.5 beam width ratio. The diameter of the longitudinal bars was 16mm, and the stirrup was 10mm. Section 3.2.1 presents the details of geometric models.

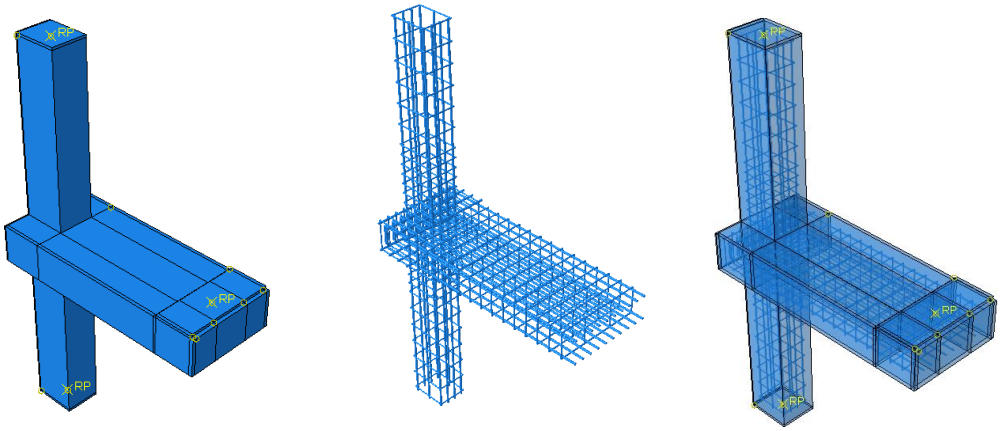

Figure 3- 4 FEM Geometrical model of specimen

3.3.3. Element Type

3.3.3.1. Concrete

In Abaqus concrete is frequently represented in finite element analysis using the general-purpose linear brick element C3D8R that has reduced integration represented by “R”. The shape functions are the same as for the C3D8 element.

The C3D8R element has the following important features:

- Reduced Integration: It uses one integration point, which lies in the center of the C3D8R element. The locking phenomenon seen in the fully integrated C3D8 element is eliminated due to this reduced integration.
- Shape Functions: its function is similar with C3D8 element.
- Node Numbering: the node numbering conforms to a particular convention referred in the Figure 3-5.
- Hourglass Control: The development of spurious zero energy modes, or hour glassing, is a possible behavior for the C3D8R element. Nevertheless, hourglass control is automatically enabled for this element as of some software versions.
- Stiffness in Bending: The C3D8R element has a tendency to be too elastic during bending.
- Concentration of Stress: At the boundary of a structure, discrete components are necessary to capture a concentration of stress.

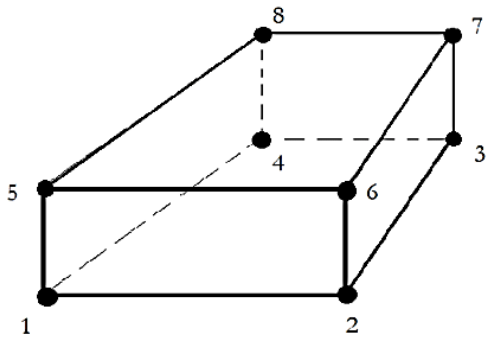

Figure 3- 5 C3D8R element numbering of nodes

3.3.3.2. Reinforcement steel

Reinforcing steel bars are modeled as 2-node linear 3D truss (T3D2) element which employed to model truss structures.

The element can be used to simulate structures that are subjected to axial loads and have three active degrees of freedom as shown in Fig.3-6.

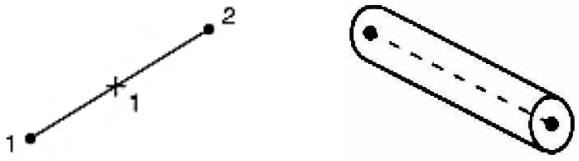

Figure 3- 6 T3D2 element numbering of nodes

Rigid elements have been set on the concrete section to apply loads. The R3D4 element type is used to model these rigid elements. A four-node tetrahedral element called R3D4 is used in ABAQUS to simulate the two-dimensional surfaces of three-dimensional rigid body. It can translate in the x, y, and z dimensions, giving each node three degrees of freedom.

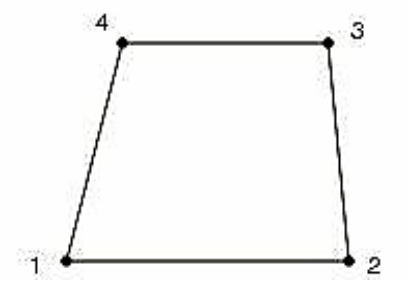

Figure 3- 7 R3D4 element numbering of nodes

3.3.4. Material Modeling

3.3.4.1.**Concrete modeling**

The damage model for concrete is a progressive model based on plasticity. It is assumed that compressive crushing and tensile cracking of the concrete material are the two primary failure modes. Two hardening variables, related to failure mechanisms under tension and compression loading, respectively, govern the development of the yield (or failure) surface. Tensile and compressive equivalent plastic stresses are that which refer to them, respectively. A wide range of fundamental models that accurately represent the behavior of concrete including its major nonlinearities and post-peak behavior in both compression and tension have been established by several investigators and are currently in widespread application.

The non-linear nature of concrete materials in compression and cracking in tension, as well as the plasticity of the steel reinforcement, must be accurately modeled using finite element modeling based on experimental verification in order to accurately simulate the behavior of reinforced concrete structures.

ABAQUS demand three fundamental models for concrete. These are:

- Concrete damage plasticity model (CDP):- replicates how concrete would react to both cyclic and monotonic loading scenarios. It specifies the inelastic deformation of concrete using a plasticity flow rule and a scalar damage variable.
- Smeared crack model (SCM):- reflects the way concrete can react to low confining pressures and monotonic straining. It takes advantage of the rotating crack concept and the isotropic hardening rule.
- Brittle cracking model (BCM):- This model represents what happens when concrete can react to extreme confining forces. The crack initiation and propagation are determined by means of a fracture energy criterion.

The CDP model combines the flow theory of plasticity with damage mechanics to accurately capture the behavior of concrete. Plasticity models alone cannot account for stiffness degradation, while damage models are not suitable for describing plastic deformations and inelastic volumetric expansion in compression.

The CDP model is based on several assumptions:

- Additive strain rate decomposition: which separates the total strain into elastic and plastic components
- Stress-strain relation: that accounts for the behavior of a material under different loading conditions
- Stiffness degradation and hardening rule: which captures the reduction in stiffness as damage accumulates
- Yield function: that defines the conditions for plastic deformation
- Flow rule: that governs plastic deformation once the yield surface is reached,
- Visco-plastic regularization: to account for time-dependent effects.

Three distinct CDP models (Carreira and Chu, 1985; CEB-FIP, 1990; CEB-FIP, 2010) has been tried to verify the finite element analysis. Out of all these models, the CEB-FIP 2010 model has been selected for this study. Since it exhibits good agreement between the FEM model and experimental specimen carried out by (H. Behnam, 2018). The behavior of the concrete is assumed to be linearly elastic until it reaches $0.4fc$m.

I. Concrete Compression Modeling

The CEB-FIP Model Code 2010 provides guidelines for modeling the compression behavior of concrete. It includes equations for the stress-strain relationship, accounts for post-peak behavior and softening, sets limits on compressive strain, considers the effect of confinement, and provides recommendations for material properties.

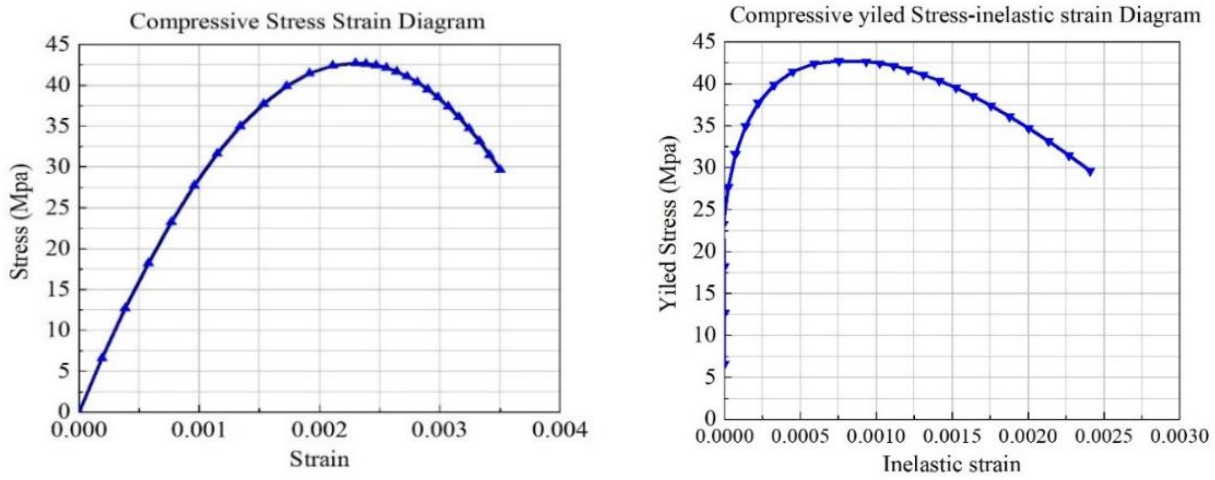

Figure 3- 8 Compressive Stress-Strain Diagrams of the Model

II. Concrete Tension Modeling

The model also offers guidelines for modeling the behavior of concrete under tension. It covers aspects such as determining tensile strength, modeling crack formation and propagation, accounting for post-cracking behavior, considering the reinforcement effect, and determining relevant material properties.

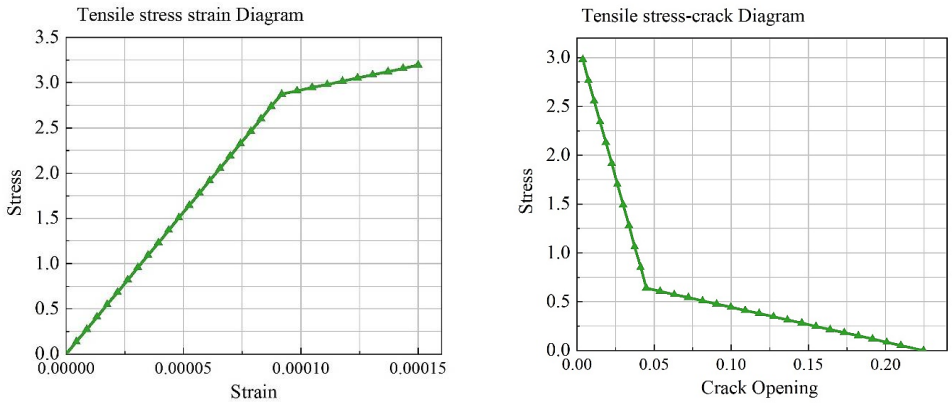

Figure 3- 9 Tensile Stress-Strain Diagrams of the Model

3.3.4.2.Reinforcement material properties

Several material models can be employed by ABAQUS to model steel bars. Including:

- Linear elasticity: This model takes the assumption that the material obeys Hooke's law and is homogenous and isotropic. Permanent deformation does not occur since the stress is proportionate to the strain. This type applies like mild steel and small deformations.
- Plasticity: This model facilitates permanent deformation of the material after it reaches the yield point. The yield criterion, flow rule, and hardening rule all influence the nonlinear stress-strain relationship. The ductile properties of metals, including stainless steel, can be represented by this model.
- Viscoelastic materials are materials that exhibit both viscous and elastic characteristics when undergoing deformation

The most common material model for steel bars is the linear elastic model, which assumes that the material behaves elastically up to its yield point. The material undergoes plastic deformation and becomes nonlinear beyond the yield point shown below by Table3-3. Plastic behavior of reinforcing steel depend on steel grade and diameter of bar previously presented in Table 3-2.

Table 3-3 Elastic Behavior of Reinforcement

Density	7850kg/m^3
Young's Modulus	200GPa
Poisson's ratio	0.3
Property	Isotropic
Material Behavior	Elasticity

Table 4-4 Plastic Behavior of Reinforcement

Reinforcement	S4	
Bar diameter (mm)	10	16
Yield strength f_y (MPa)	511	558
Ultimate strength f_u (MPa)	620	642
Yield strain (%)	0.255	0.279
Ultimate strain (%)	12	9

3.3.5. Meshing and mesh sensitivity

The mesh sensitivity analysis has been performed for different sizes of the mesh such as 40mm, 50mm and 60mm element sizes for one sample. As a result of exhibited good convergence, a fine mesh size of 50mm is selected for subsequent finite element analysis. All samples have meshed with tetrahedral-shaped elements.

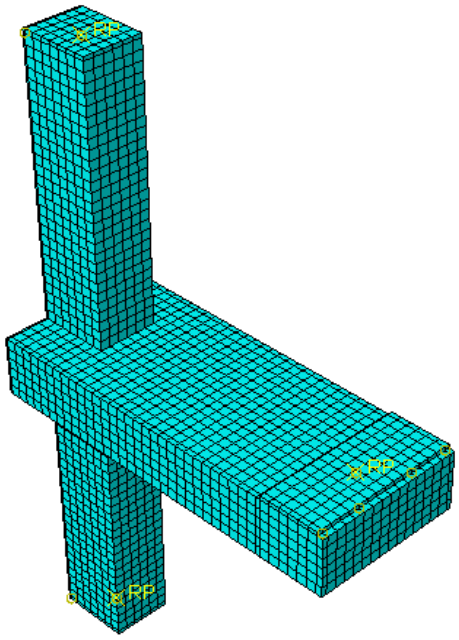

Figure 3- 10 Meshed finite element model

3.3.6. Interaction Modeling

In Abaqus, interaction modeling is the process of specifying how various model sections interact with one another under different types of loading. The modeling of interactions within a system involves taking into account various factors that affect how the model deforms and distributes

stress. These factors include elements like fasteners, connectors, and contacts, which play a role in determining the behavior of the system under consideration.

It is important to select an accurate model to obtain a sufficient force transmission between the interacting surfaces and practical modeling of the real contact behavior. In this FE model three different types of interactions are used to simulate the interface action between pairs of interacting surfaces.

The embedded region constraint provided by the ABAQUS Standard was used to specify the bonding of reinforcing bars with concrete. This interaction involves the reinforced bar acting as an embedded element and the surrounding concrete acting as the host element. In the reinforced concrete model, "tension stiffening" is specified to approximate load transfer across cracks through the rebar. This model indirectly represents the processes commonly associated with the reinforcement-concrete interface, like bond slip and dowel action.

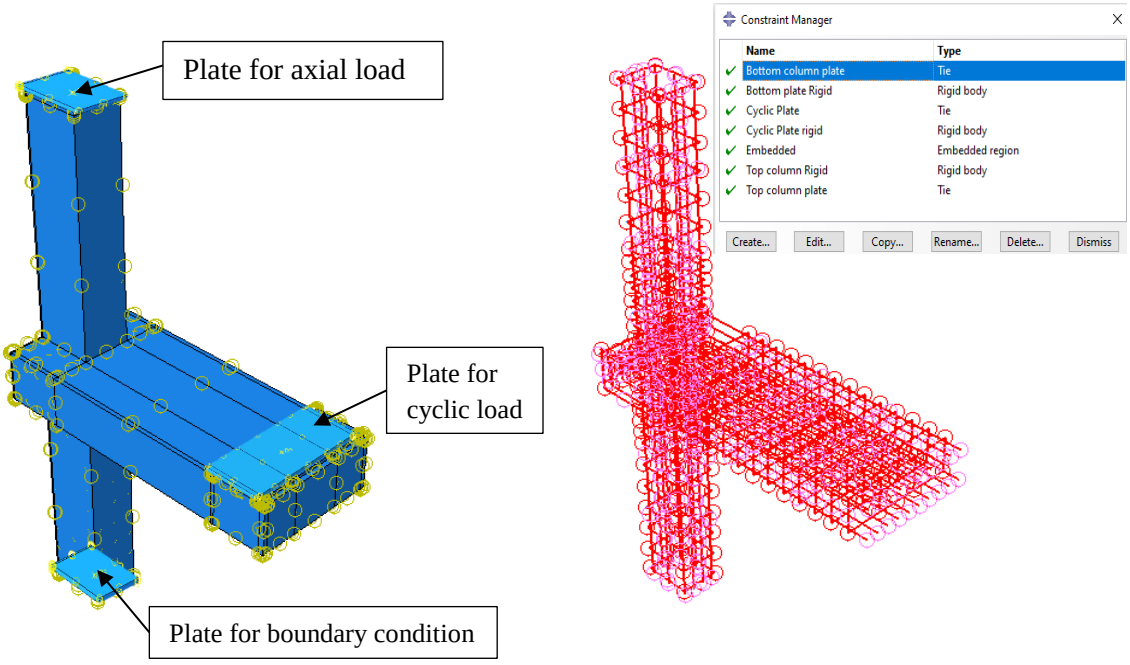

Figure 3- 11 Interactions between components of the joint model

ABAQUS/Standard uses the configuration of a model to identify that slave nodes are precisely contacting the master surface at the beginning of the analysis when a contact pair employs the tied

contact formulation. Next, ABAQUS/Standard creates constraints on the master surface between these slave nodes and adjacent nodes.

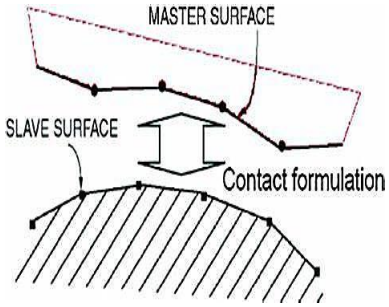

Figure 3- 12 Contact formulation in Abaqus

In this mode, the contact between a stiff plate and the concrete is defined by tie type of interaction. The load imposed on the stiffer plate will be distributed uniformly to the less stiff portion of the concrete. The rigid plate serves as the master surface and the other as the slave surface based on their stiffness. To establish an interaction between the rigid body elements and the point of load application on the rigid plates, this investigation uses rigid body contact.

3.3.7. Boundary Condition and Loading

In ABAQUS, boundary conditions pertain to the constraint imposed on a model at its boundaries or interfaces. These limitations encompass prescribed loads, fixed displacements, and contact interactions. After thorough examination and simulation of the experimental data, the fixed support boundary condition shown in Fig.3-13 has been selected for this study.

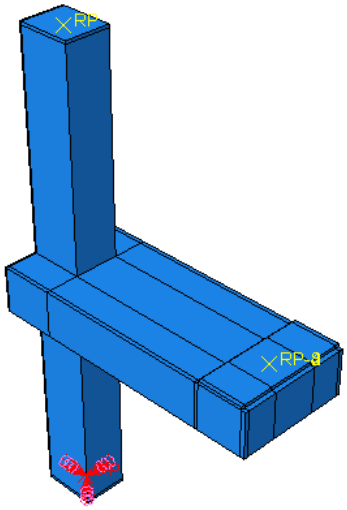

Figure 3- 13 Boundary condition of model

The process of load application involves the development of two load phases. A set of loads that are applied to the model at a particular interval or time during the analysis is referred to as a load step. The column was subjected to an axial compressive load of 480 kN using a rigid plate.

Cyclic displacement (Δ) was introduced to the top of the wide beam. There are three iterations of the cyclic displacements with single displacement, and the time interval. The cyclic displacements are repeated three times for each displacement, with a set time interval between each cycle of 0.2 seconds.

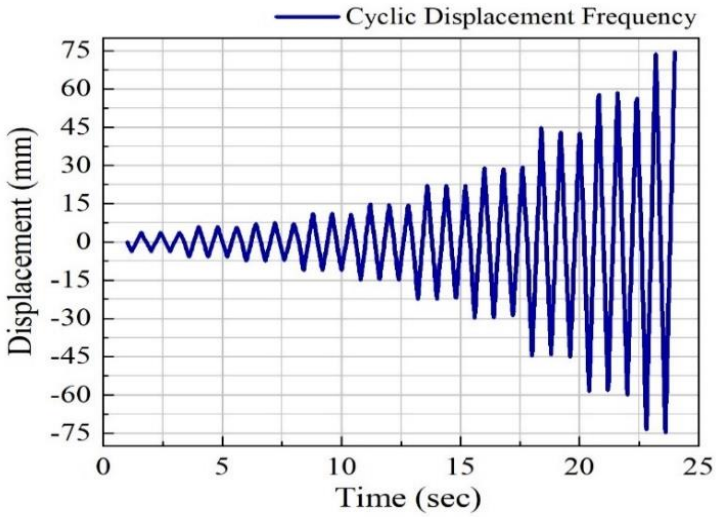

Figure 3- 14 FEM cyclic displacement schedule

In order to accelerate the convergence rate, an automatic incremental approach was implemented, utilizing a smaller time step size and a larger maximum number of increments. To apply the boundary conditions similar to the test setup, first, the surfaces of the column end attached to the surfaces of the rigid plate, and then after the plate and reference points are rigidly connected, the boundary conditions will be applied to these reference points.

3.4. Parameters

The parameters selected for this investigation were based on the need for enhancing transverse beam torsional capacity, which is expected instantly improve shear strength of wide beam column joints according to previously conducted researches.[33]

3.4.1. Spacing of Transverse Reinforcement (Stirrup)

The use of transverse reinforcement (stirrups) is essential in reinforced concrete (RC) beams to resist shear and torsion forces. Stirrups play a crucial role in providing confinement to the concrete core, preventing the propagation of diagonal cracks, and enhancing the ductility of beam and ability to dissipate energy. These factors collectively improve the torsional capacity of RC beams. It is important to note that the performance of stirrups is influenced by factors such as their spacing and material properties. So, in this study, both parameters have been studied [100mm-200mm].

3.4.2. Yield strength of Transverse Reinforcement

The yield strength of the reinforcement bars is a crucial material property that determines their ability to withstand loads. The strength of the transverse bars directly affects the capacity of stirrups to resist torsional shear stresses and inhibit the formation and propagation of diagonal cracks in the concrete. Therefore, the strength of the transverse bars serves as a significant parameter that reflects the influence of material properties on the performance of stirrups. The selection of the yield strength range for the study is based on practical availability and common practices [400-500 MPa].

3.4.3. Longitudinal Reinforcement Ratio

Longitudinal reinforcement bars resist torsion by generating tensile stresses. Design considerations include the quantity and distribution of these bars. With sufficient reinforcement volume and arrangement, the beam will demonstrate a ductile failure mode as the concrete undergoes crushing, avoiding brittle failure. During the cracking stage, the longitudinal reinforcement carries the majority of the torsional moment. In this stage, the reinforcement can sustain additional loads on the beam by yielding and undergoing plastic deformation. This phase is known as the post-cracking stage and it significantly contributes to the torsional capacity of the beam [0.0053 - 0.0209].

3.4.4. Yield Strength of Longitudinal Reinforcement

An RC beam undergoes twisting as it is subjected to torsion. The concrete and reinforcement bar in the beam resists the shear forces caused by this action. The amount of stress the longitudinal reinforcement can withstand before yielding or plastically deforming is determined by its yield strength.

The yield strength of longitudinal reinforcement affects how shear and bending forces interact with it. It contributes in the resistance of the combined shear, bending, and torsion forces acting on a beam. A larger yield strength is expected to enable the reinforcement to withstand higher total stresses, increasing the overall capacity of the beam to support loads [400 -600 MPa].

3.4.5. Compressive Strength of Concrete

The shear forces induced by twisting are resisted by the concrete together with reinforcement bar in the beam. The compressive strength of a concrete determines the ability to withstand shear force before cracking. It plays a crucial role in resisting torsion in reinforced concrete (RC) beams. Torsional forces can lead to cracking and failure if not adequately resisted. The compressive strength of concrete directly affects the ability of the beam to withstand these torsional forces. It also affects the development of cracks and maintaining the structural integrity of the beam under torsional loading [25MPa – 40MPa].

3.4.6. Diameter of longitudinal bar

The diameter of the longitudinal bar also affects the angle of the compression struts in the concrete, which can influences the torsional strength. On the other hand, it affects the ratio of the shear span to the effective depth (a/d), which controls the performance of RC beams in shear. Additionally, it influences the crack control and distributions in beams. In this study effect of diameter in concrete damage has been investigated. The range of study is arranged based on practical availability [14, 16, 20, 24] mm.

3.5. Latin Hypercube Sampling (LHS)

In parametric studies, the Latin Hypercube Sampling (LHS) technique is an approach for efficiently exploring the parameter space. LHS ensures a more representative and evenly distributed sampling of the parameter ranges compared to traditional random sampling methods. The technique partitions the parameter space into equally sized intervals and selects a single value from each interval, ensuring that each parameter value is uniquely paired with others. This creates a diverse and stratified sample set that covers the entire parameter space without redundancy. This technique is particularly valuable in parametric studies where a large number of input parameters need to be evaluated to understand their effects on the system under investigation.

The selection of specimen combinations for this research study was carried out using the Latin Hypercube Sampling (LHS) method. The specific details regarding the samples used in the parametric study can be shown in Table 3-5. The values obtained from LHS for two parameters have been rounded to whole numbers as a result of specific factors. When sampling the diameter, the values tend to be approximated to the currently available sizes. This is because the diameter options in practical applications are typically limited to certain discrete sizes and the sampled values reflect this constraint. The approximation of whole numbers in LHS sampling for spacing parameters is attributed to the practical considerations.

Table 3-4 Detailing of the specimens for parametric study

Specimen	Diameter (mm)	fc (MPa)	Spacing (mm)	fys (MPa)	fy (MPa)	As (ρ)
14M1	14	35.4496	170	498.351	501.233	0.0053037
14M2	14	30.4044	140	421.447	515.824	0.0087555
14M3	14	27.6981	110	409.32	499.879	0.0065037
14M4	14	29.7169	185	482.694	520.369	0.0079655
14M5	14	33.063	125	418.965	407.068	0.0056937
14M6	14	39.6606	185	433.245	587.556	0.0060103
14M7	14	38.0939	190	429.687	411.358	0.0055770
14M8	14	26.2124	105	498.624	579.978	0.0054133
14M9	14	36.6143	175	414.544	582.395	0.0060521
14M10	14	28.392	140	479.685	486.957	0.0056809
14M11	14	26.7964	185	489.972	520.548	0.0061034
14M12	14	26.5331	150	495.122	591.855	0.0058037
14M13	14	34.9891	135	469.899	430.011	0.0071296
14M14	14	28.5711	130	497.774	510.654	0.0059037
14M15	14	35.7613	150	481.897	419.758	0.0060037
14M16	14	34.3916	120	493.244	588.669	0.0085556
14M17	14	25.2039	155	479.734	414.398	0.0099815
16M1	16	37.5516	160	406.195	532.201	0.0130370
16M2	16	29.5428	135	415.798	524.069	0.0093122
16M3	16	28.0954	100	487.253	479.966	0.0073672

16M4	16	38.1666	180	476.258	440.257	0.0074497
16M5	16	29.2816	115	490.447	481.967	0.0111746
16M6	16	25.7677	190	425.574	418.969	0.0069697
16M7	16	37.0825	180	480.447	550.322	0.0073497
16M8	16	32.2091	130	475.399	549.826	0.0167619
16M9	16	38.8828	170	430.074	537.352	0.0148995
16M10	16	34.3621	180	469.922	584.369	0.0130370
16M11	16	31.6494	190	403.988	590.557	0.0073774
16M12	16	35.1141	105	411.351	587.464	0.0186243
16M13	16	31.9098	160	441.234	589.354	0.0167619
16M14	16	39.9118	160	477.695	469.991	0.0185954
16M15	16	25.3862	170	496.92	443.558	0.0073647
16M16	16	31.3798	155	462.301	577.824	0.0112746
20M1	20	39.3524	185	469.099	580.011	0.0116402
20M2	20	33.447	145	435.208	583.996	0.0174603
20M3	20	29.0557	115	441.085	429.355	0.0203704
20M4	20	32.7557	190	473.488	507.986	0.0145503
20M5	20	33.1855	110	489.509	518.693	0.0144950
20M6	20	33.8416	140	471.872	428.869	0.0157503
20M7	20	27.2062	165	469.999	568.997	0.0174603
20M8	20	30.839	190	488.297	469.992	0.0116352
20M9	20	26.9482	185	467.987	431.779	0.0145492
20M10	20	38.5279	120	477.201	573.975	0.0175303
20M11	20	30.9935	190	493.011	433.291	0.0155502
24M1	24	37.3047	185	450.279	546.621	0.0208962
24M2	24	30.2355	190	499.101	599.012	0.0209524
24M3	24	36.2923	180	486.3	477.992	0.0167619
24M4	24	36.0193	190	481.799	402.024	0.0208999

3.6. Calibration and plastic parameters

Calibration analyses are commonly employed in FE software to assess how changing material characteristics affect a numerical model through the comparison with experimental results.

Consequently, in order to ensure the accuracy of the nonlinear finite element model of the beam-column joints, the influence of changing geometric and material input parameters, such as the dilation angle and viscosity parameter, in the essential equations of the damaged plasticity model have to be calibrated. Later on nonlinear finite element simulations are carried out on each beam-column joint sample using the calibrated nonlinear finite element model parameters.

3.6.1. Mesh

The mesh sizes used in a numerical simulation play a critical role. The mesh represents the structural and material properties of the analyzed structure, influencing its response to different loads and conditions. In finite element modeling, strain localization affects only a few sections and lets other sections be unloaded, hence the numerical model depends on the mesh size. A finer grid or mesh yields a more accurate result. However, increasing the fineness of the mesh leads to longer computation times due to the increased complexity of the calculations. The ideal situation of the finite element method is that the solution will converge with a reasonable amount of line refinement.

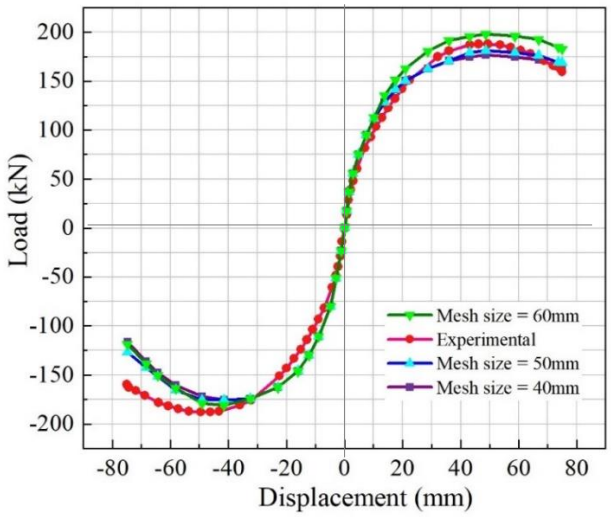

Figure 3- 15 Different Mesh Sizes Calibration

The mesh size for the samples in this finite element analysis is selected from among the three mesh sizes. After calibrating these three mesh sizes (40, 50, and 60 mm) to approximately match the experimental curve as presented in Fig 3-15 , it has been determined that both 40 mm and 50 mm mesh sizes yield satisfactory outcomes, but considering computational time, the 50 mm mesh size has been chosen.

3.6.2. Dilation Angle

When an element deviates as due to of applied stress, its inclination is known as the dilation angle (Ψ), it describes the volumetric change that occurs in a concrete particle under shear deformation. Its values commonly fall between (25–50) degrees based on the range that earlier researches employed.

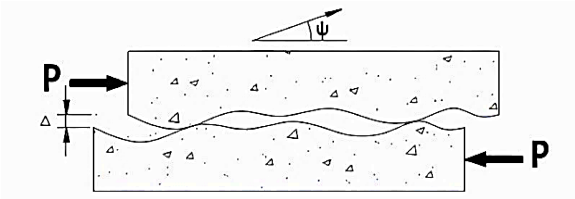

Figure 3- 16 Dilation Angle (Ψ),

The volumetric strain that results from plastic deformation is governed by the dilation angle.[34] As Figure 3-16 shown the quasi-conical shape of the stress transmission is also determined by its slope, which is the failure surface.

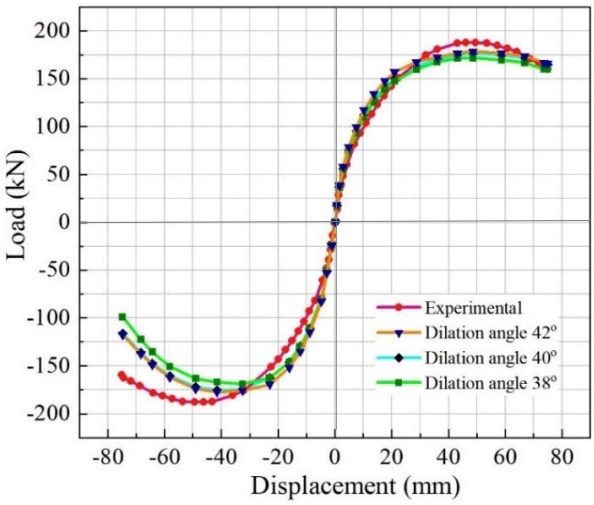

Figure 3- 17 Different Dilation Angle Calibration

As the calibration analysis shown in Figure 3-17, the dilation angles of 38°, 40°, and 42° yield the best prediction with a sufficient number of iterations. An ideal alignment occurs when the **40°** dilation angle is consistent with other plastic properties, such as viscosity and mesh size, resulting in an optimal match.

3.6.3. Viscosity

The concrete damaged plasticity (CDP) model in ABAQUS/Standard is regularized by a viscosity parameter. The CDP model takes into account the degradation of elastic stiffness caused on by plastic straining in both compression and tension, and it is predicated on the idea of isotropic damage. A viscosity parameter can be adjusted to allow the material to pass the plastic potential surface in order to improve the solution and address convergence difficulties. When the dilation angle is maintained constant, raising the viscosity parameter enhances the capacity of the beam and deflection.

Three μ values (0.01, 0.002, and 0.003) are used in this study to calibrate the lateral load-displacement behavior. Figure 3-18 illustrates that the variations resulting from varying viscosity have no significant effect. Rather, varying viscosity parameter values affect the analysis duration. So taking this into account and considering better correlation with the experimental data the value **μ=0.003** is used for all samples in this investigation.

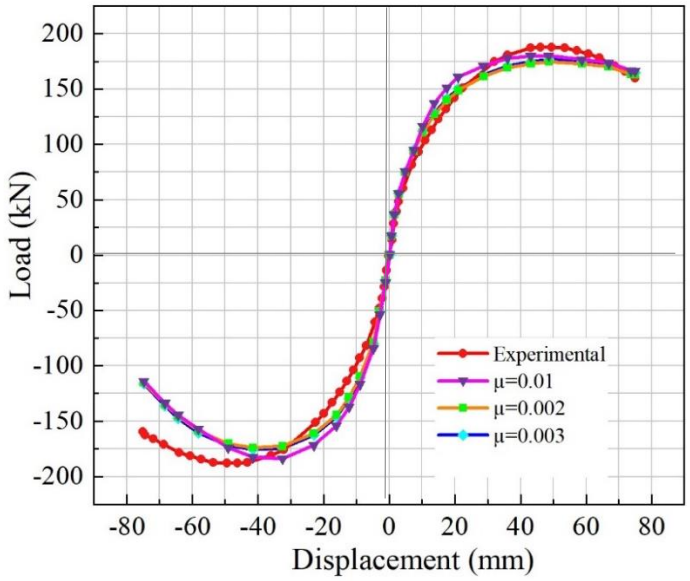

Figure 3- 18 Different Viscosity Parameter Calibration

3.6.4. Shape factor

In the ABAQUS concrete damaged plasticity model, the form of the yield surface is determined by the parameter shape factor *Kc* which measures the efficacy of an element in the mesh.

Tetrahedral and triangular elements are the only ones for which the shape factor criterion is available. The shape factor is a number between 0 and 1, where 0 denotes a degenerate element and 1 represents the ideal element shape. The determination of the value of *Kc* was based on a range established through the collective study of multiple authors who conducted finite element investigations on concrete structures. Three different KC values are examined in this study 0.55, 0.667 and 0.75. Among these values, Kc=0.667 was selected as it provided the best fit to the experimental curve as shown in Fig. 3-19.

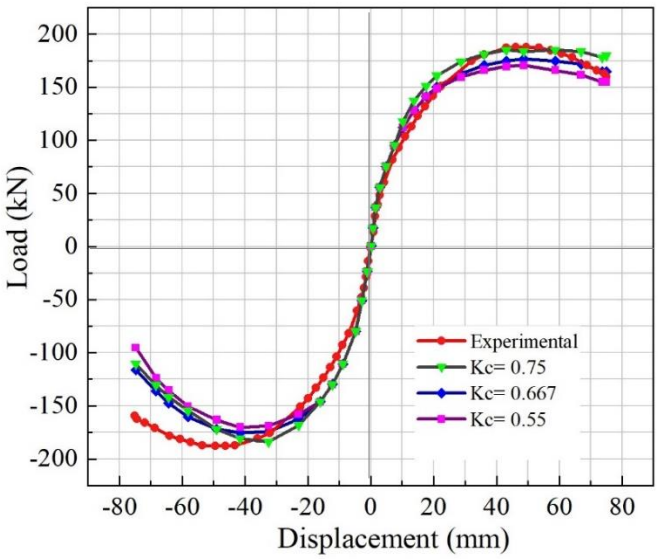

Figure 3- 19 Different Shape Factor Parameter Calibration

3.7. Validation of the Nonlinear Finite Element Model

As shown in Figure 3-2, a reinforced concrete wide-beam column joint subjected to cyclic loading in addition to axial loading. The accuracy of the nonlinear finite element model is evaluated by comparing the nonlinear finite element analysis results of these samples with the corresponding experimental results for lateral load-displacement capacity, ultimate load and failure pattern. Comparisons based on the lateral load-displacement responses of the samples as determined by nonlinear finite element analysis and reported from experimental test results are discussed in the next subsection.

3.7.1. Lateral load-displacement relationship

The load-displacement hysteresis and envelope curves obtained from nonlinear finite element analysis compared with the experimental results of the specimen are shown in Figure 3-20 (a) and (b), respectively. The result validates the numerical FE method implemented using ABAQUS software. The load–displacement curve shows a good agreement between the results of FEM analysis and actual values reported by H. Behnam (2018). Based on the experimental result maximum load that the RC wide beam-column joint can sustain is 185.8 KN, while the results given by ABAQUS predict this parameter as 173.8 KN. This shows the average peak lateral load predicted by the numerical model is 6.9% lower than the peak lateral load reported from the experimental result.

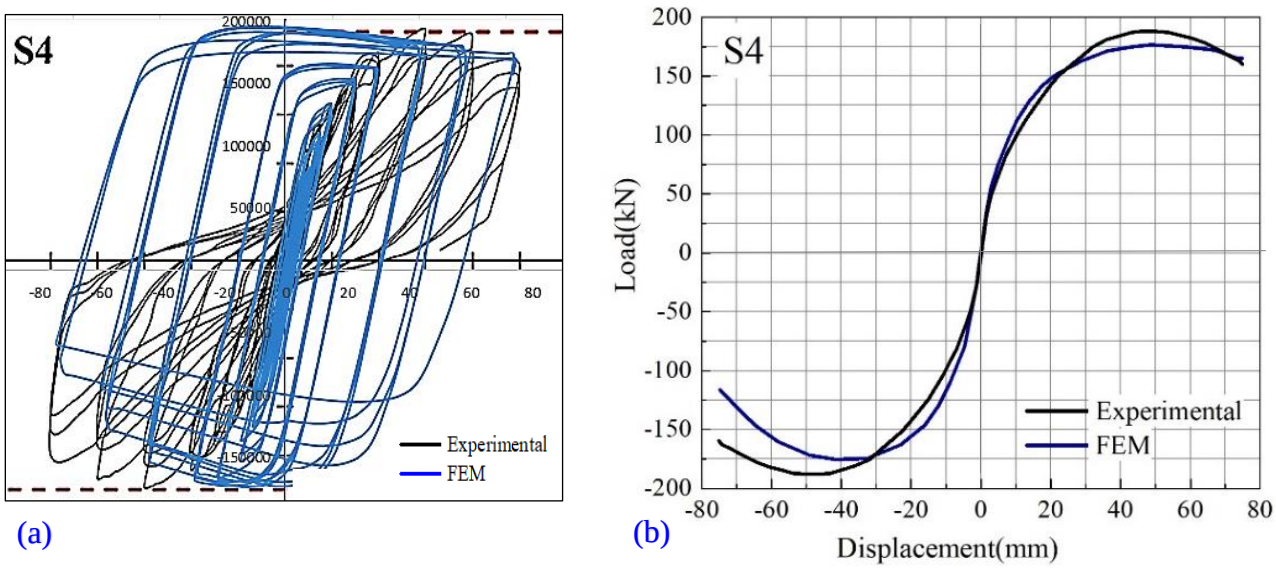

Figure 3- 20 Hysteresis loops and envelop curve of validation

The pinching effect in the cyclic load displacement hysteresis curve is significant when comparing Abaqus simulations with experimental data. It occurs due to material nonlinearity and stiffness and strength degradation during cyclic loading. In experimental tests, the pinching effect is observed as the hysteresis loop narrows or "pinches" inward, indicating energy dissipation and damage accumulation. Table 3-5 presents a comparison between the error and accuracy of the FEA predictions and the experimental test results (both positive and negative values) for the validation specimen (S4).

Table 3-5 Comparison of FEA and experimental lateral load carrying capacity of specimen

	Load Capacity V(kN)		Prediction	
	Experimental	FEM	Accuracy (%)	Error (%)
Positive(+)	189	176.8	93.1	6.90
Negative(-)	185.8	172.7	92.41	7.59
Average	187.4	174	92.77	7.23

3.7.2. Failure mode and patterns

Determining the maximum capacity alone is not sufficient to describe the complete behavior of structural elements. Especially for numerical simulations, the model should be able to capture and simulate various types of failures and their associated deformations. Therefore, in the following subsections, Figure 3-21 presents a comparison of the failure mode of samples obtained by nonlinear finite element analysis and those reported from experimental test results. Table in APPENDIX-A presents a comprehensive comparison of the displacement ductility index values obtained from experimental tests and those predicted through FEM analysis. The close agreement between the two sets of data suggests that the FEM model adequately captures the nonlinear behavior, deformation capacity and energy dissipation characteristics of the structure.

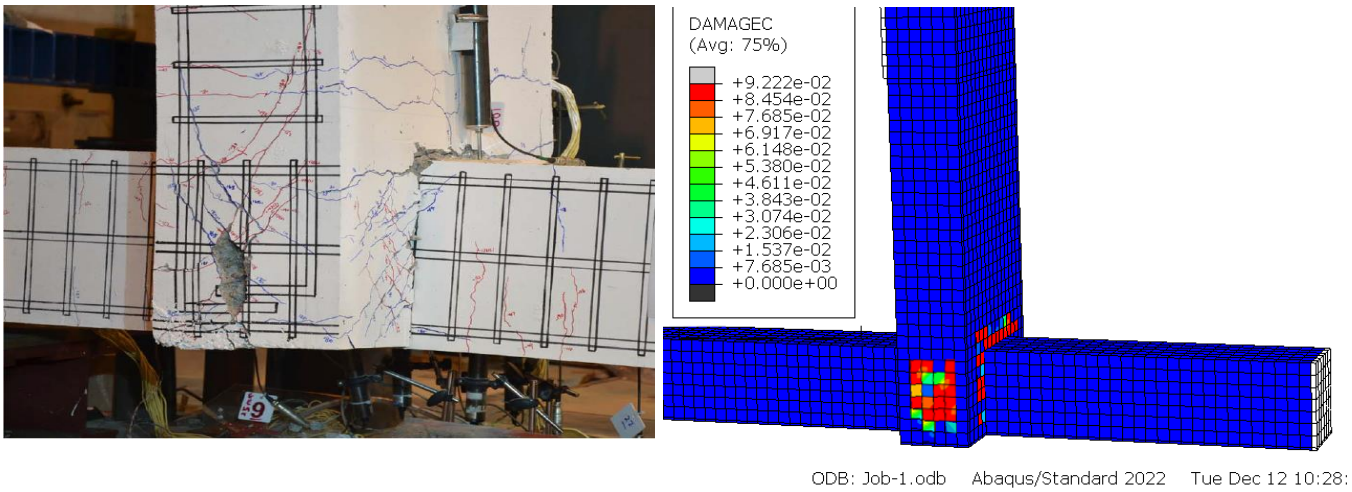

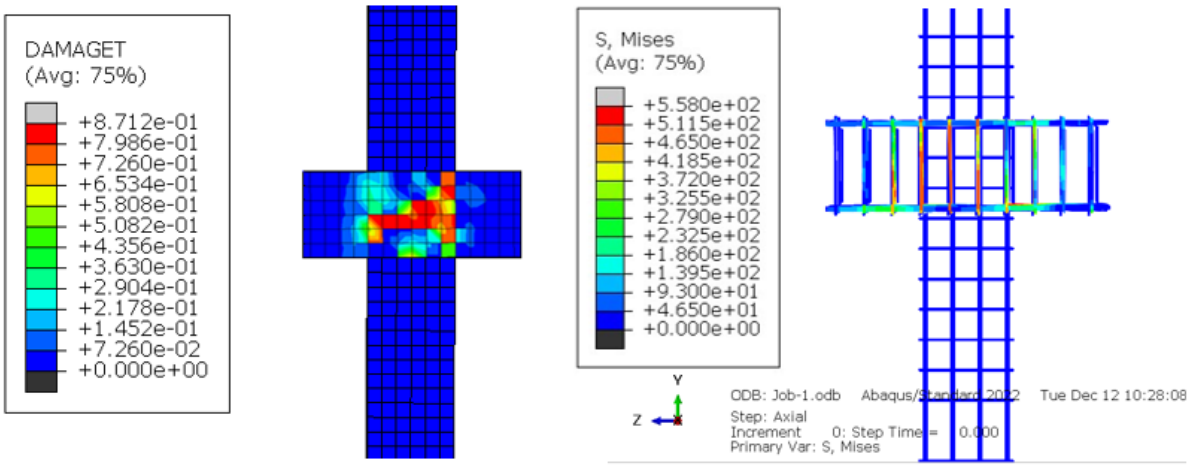

Figure 3- 21 Comparison of FEA and experiment test damage results

4. RESULT AND DISCUSSION

4.1. Introduction

In this chapter the parametric analysis of samples that study the effect of compressive strength of concrete, longitudinal bar reinforcement ratio, stirrup spacing, yield strength of transverse reinforcement, longitudinal bar diameter and yield strength of transverse beam in the shear strength of wide beam column joint will be presented. Regression analysis was conducted following the parametric analysis to propose a formula that can be integrated with the existing expected shear strength formula provided by the ACI, addressing transverse beam parameters as well as their contribution to shear strength of the joint. Then, sensitivity analysis was carried out to determine corresponding degrees of influence. Finally, selected cases were examined and discussed based on their cyclic load hysteresis curve, envelope curve, ductility and concrete damage.

4.2. Parametric Study Result and Discussion

After validation of the FE analysis, an investigation was conducted on RC wide beam-column joints through a parametric study involving different parameters. The range value of these parameters is selected based on the code specification and practical use. The study investigated how various parameters affected the lateral load-carrying capacity of RC wide beam columns.

Table 4- 1 Analysis Result summary

No.	Specimen Label	Diameter (mm)	f_c (MPa)	Spacing (mm)	Fys (MPa)	fy (MPa)	A_s ratio	V_j (kN)
1	14M1	14	35.4496	170	498.351	501.233	0.0053037	176.415
2	14M2	14	30.4044	140	421.447	515.824	0.0087555	169.885
3	14M3	14	27.6981	110	409.32	499.879	0.0065037	168.351
4	14M4	14	29.7169	185	482.694	520.369	0.0079655	168.935
5	14M5	14	33.063	125	418.965	407.068	0.0056937	167.188
6	14M6	14	39.6606	185	433.245	587.556	0.0060103	176.636
7	14M7	14	38.0939	190	429.687	411.358	0.0055770	172.184
8	14M8	14	26.2124	105	498.624	579.978	0.0054133	170.120
9	14M9	14	36.6143	175	414.544	582.395	0.0060521	174.561
10	14M10	14	28.392	140	479.685	486.957	0.0056809	166.625
11	14M11	14	26.7964	185	489.972	520.548	0.0061034	166.648
12	14M12	14	26.5331	150	495.122	591.855	0.0058037	169.104
13	14M13	14	34.9891	135	469.899	430.011	0.0071296	176.222
14	14M14	14	28.5711	130	497.774	510.654	0.0059037	169.820

15	14M15	14	35.7613	150	481.897	419.758	0.0060037	178.162
16	14M16	14	34.3916	120	493.244	588.669	0.0085556	176.531
17	14M17	14	25.2039	155	479.734	414.398	0.0099815	170.445
18	16M1	16	37.5516	160	406.195	532.201	0.0130370	179.112
19	16M2	16	29.5428	135	415.798	524.069	0.0093122	171.860
20	16M3	16	28.0954	100	487.253	479.966	0.0073672	171.086
21	16M4	16	38.1666	180	476.258	440.257	0.0074497	173.312
22	16M5	16	29.2816	115	490.447	481.967	0.0111746	174.300
23	16M6	16	25.7677	190	425.574	418.969	0.0069697	167.389
24	16M7	16	37.0825	180	480.447	550.322	0.0073497	173.605
25	16M8	16	32.2091	130	475.399	549.826	0.0167619	178.741
26	16M9	16	38.8828	170	430.074	537.352	0.0148995	180.309
27	16M10	16	34.3621	180	469.922	584.369	0.0130370	177.584
28	16M11	16	31.6494	190	403.988	590.557	0.0073774	170.406
29	16M12	16	35.1141	105	411.351	587.464	0.0186243	181.123
30	16M13	16	31.9098	160	441.234	589.354	0.0167619	176.150
31	16M14	16	39.9118	160	477.695	469.991	0.0185954	183.400
32	16M15	16	25.3862	170	496.92	443.558	0.0073647	169.748
33	16M16	16	31.3798	155	462.301	577.824	0.0112746	176.018
34	20M1	20	39.3524	185	469.099	580.011	0.0116402	180.314
35	20M2	20	33.447	145	435.208	583.996	0.0174603	178.767
36	20M3	20	29.0557	115	441.085	429.355	0.0203704	181.273
37	20M4	20	32.7557	190	473.488	507.986	0.0145503	177.101
38	20M5	20	33.1855	110	489.509	518.693	0.0144950	180.630
39	20M6	20	33.8416	140	471.872	428.869	0.0157503	178.770
40	20M7	20	27.2062	165	469.999	568.997	0.0174603	173.119
41	20M8	20	30.839	190	488.297	469.992	0.0116352	172.949
42	20M9	20	26.9482	185	467.987	431.779	0.0145492	172.127
43	20M10	20	38.5279	120	477.201	573.975	0.0175303	182.528
44	20M11	20	30.9935	190	493.011	433.291	0.0155502	175.138
45	24M1	24	37.3047	185	450.279	546.621	0.0208962	182.680
46	24M2	24	30.2355	190	499.101	599.012	0.0209524	181.788
47	24M3	24	36.2923	180	486.300	477.992	0.0167619	178.063
48	24M4	24	36.0193	190	481.799	402.024	0.0208999	182.350

The results of the parametric study revealed that the transverse beam parameters has a role in determining the shear strength of the joint, regardless of changes in the wide beam parameters. This highlights the importance of considering these parameters when assessing shear strength.

The shear strength predictions made by ACI did not explicitly account the effect of transverse beam parameters. The expected shear strength was primarily influenced by the wide beam parameters. It is calculated using actual material strength. The lateral load capacity ($V_{b,e)}$ is determined by Eq.4.2 analyzing the force and moment equilibrium. The nominal flexural strength (M_{nb}) is calculated by Eq.4.1 according to ACI 318-14. Detail procedure outlined on ANNEIX D.

$$M_{nb} = \phi A_s f_y (d - a/2) \quad \text{..... 4.1}$$

Where: ϕ : Reduction factor of strength [0.65 to 0.9]

A_s: Longitudinal reinforcement area of tension

f_y: Reinforcement yield strength

d: effective depth of beam

a: in the compression zone depth of the equivalent rectangular stress block

$$V_{be}^{ACI} = \frac{M_{nb}}{L_b} \quad \text{..... 4.2}$$

L_b: refers the distance between the loading point and the face of the column

To improve the accuracy of shear strength predictions in the joints, a formula that incorporates the transverse beam parameters has been proposed by using regression analysis. This method can show that variations in the dependent variable are correlated with changes in one or more of the factors explaining the dependent variable. To achieve this, it basically correlates a best-fit line and observes the distribution of the data around it. The regression statistics including R square value presented by Table 4- 2 that shows how the dependent and independent variables are correlated.

Table 4- 2 Regression Statistics

Regression Statistics	
Multiple R	0.9428
R Square	0.8899
Adjusted R Square	0.8786
Standard Error	1.7064
Observations	48

The shear capacity contribution from transverse beam ($\mathbf{V_{jt}}$) obtained from analysis is expressed by a general formula Eq.4.3

$$V_{jt} = -45.905 + 0.66 * fc - 0.0257 * S + 0.0238 * fys + 607.2485 * \rho \quad \text{..... 4.3}$$

Where

$\mathbf{f_c}$: Concrete compressive strength in (MPa)

S: Spacing of stirrup in (mm)

$\mathbf{f_{ys}}$**:** Yield strength of stirrup reinforcement in (MPa)

ρ: Longitudinal reinforcement ratio

Modified expression Eq. 4.4 resulting in more precise predictions of shear strength since it takes into account both wide beam and transverse beam parameters, V_m becomes:

$$V_m = V_{be}^{ACI} + V_{jt} \quad \text{.....4.4}$$

Where

V_m Modified shear strength prediction

V_{be}^{ACI} Shear strength prediction by ACI

V_{jt} Shear capacity contribution from transverse beam

4.2.1. Sensitivity Analysis

Sensitivity analysis is a valuable technique employed to assess how alterations in input variables influence the output of a model and to evaluate the importance of each input variable in determining the overall output. When conducting parametric studies, it can help to identify the most critical parameters within a model, establish the range of values for which the model remains valid, and recognize the parameters that exert the greatest influence on the output of model.The degree of sensitivity for each random variable is indicated by the squared value of the partial coefficient of correlation (r_p^2). The input values for sensitivity analysis are obtained from Table 4-1. In the case of uncertainty analysis, the sensitivity factor α_i, calculated using the first-order approximation second-moment method. The sensitivity factor can be calculated by Eq.4.5.

$$\alpha_i = \frac{\partial F}{\partial x_i}\frac{\bar{x}_i}{\bar{F}} \qquad (i = 1,2,3,\ldots,n) \quad \text{.....4.5}$$

where,

α_i :sensitivity factor of random variable i

F :function with statistical variations

$\overline{F}$:mean of F

The sensitivity factor α_i serves as an index that quantifies the extent to which the uncertainty in the variable x_i influences the uncertainty in F.

Table 4-3 Sensitivity and uncertainty factors

Random variables (i)	COV_i	Sensitivity factor (α_i)	Percentage of influence
f_c	13.435	2.05121	49.37%
s	18.727	-1.05426	25.38%
A_s	45.185	0.66534	16.02%
f_{ys}	6.525	0.38364	9.23%

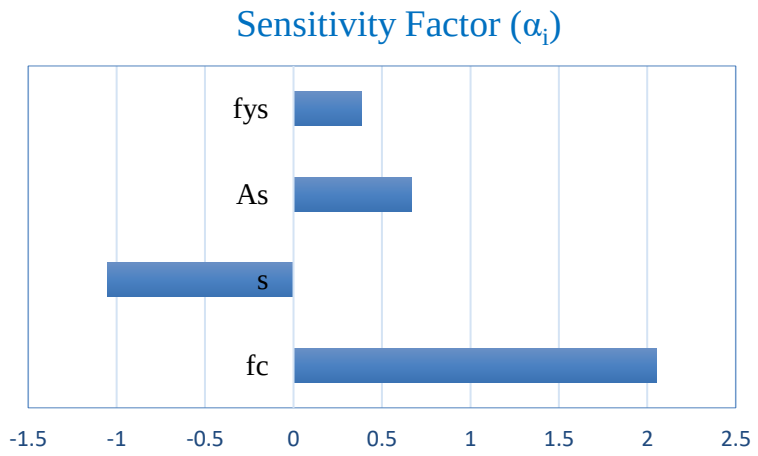

Figure 4- 1 Graphical representation of sensitivity analysis

The results of the sensitivity analysis that presented in Fig.4-1 highlight the varying degrees of influence that different parameters have on the shear strength of the wide beam column joint.

The concrete compressive strength emerges as the most influential parameter, explaining **49.37%** of the shear strength variation. This can be attributed to the direct impact of concrete compressive strength on its ability to resist applied loads and withstand shear forces.

The spacing of stirrup is identified as the second most influential parameter, accounting for **25.38**% of the shear strength variation. Stirrups effectively confine the concrete core and restrain the diagonal cracks that occur under shear loading. A smaller spacing between stirrups increases the number of stirrups per unit length, thereby improving shear strength of the joint. The longitudinal reinforcement ratio is recognized as the third most influential parameter, explaining **16.02%** of the shear strength variation. A higher reinforcement ratio enhances the joint's capacity to resist shear forces by increasing overall stiffness and strength. Conversely, the yield strength of stirrup reinforcement is found to be the least influential parameter, accounting for **9.23%** of the shear strength variation. While the yield strength of stirrups affects their ductility and ability to deform plastically, it has a relatively smaller effect compared to rest parameters. This suggests that variations in the yield strength of stirrup reinforcement have a comparatively lesser effect on the shear strength of the joint when compared to the concrete compressive strength, spacing of stirrup, and longitudinal reinforcement ratio.

For a detailed discussion, two cases have been selected: Case 14M9 and Case 16M5. These cases have been chosen based on their similarities in ultimate lateral load capacity but differences in combination parameters. The objective is to analyze the hysteresis curves, ductility, and concrete damage of these cases to understand the effect of these parameters on the behavior and performance of wide beam-column joints.

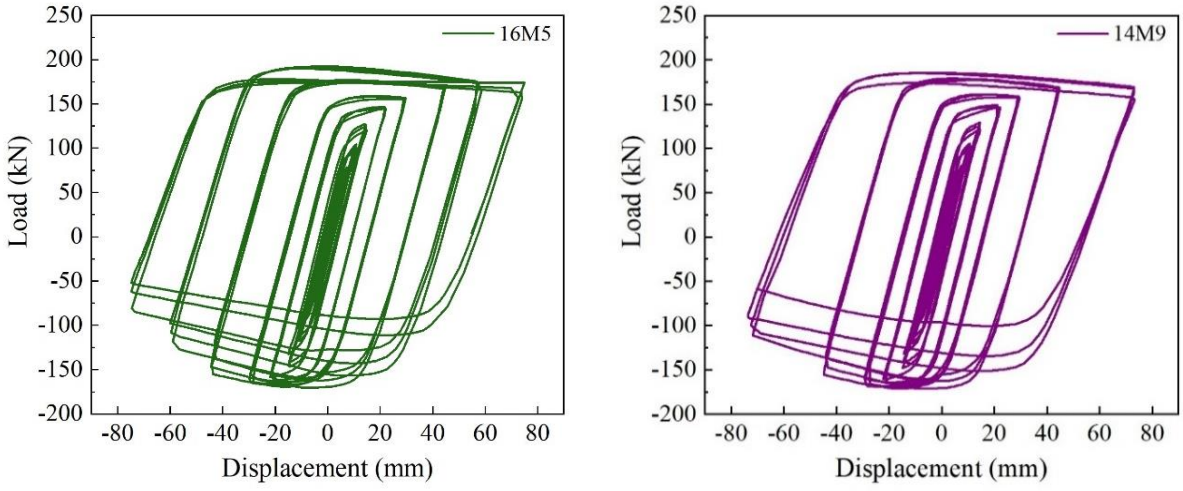

Figure 4- 2 Hysteresis Curve for 16M5 and 14M9

These cases exhibit notable differences in different parameters. In Case 14M9, the concrete grade is relatively high at 36.614 MPa, accompanied by a low reinforcement ratio of 0.00605 and a yield strength of 414.544 MPa. Additionally, the stirrup spacing in this case measuring 175 mm. On the other hand, Case 16M5 features a comparatively lower concrete grade of 29.282 MPa, a higher reinforcement ratio of 0.0112, and a yield strength of 490.447 MPa. The stirrup spacing in this case is reduced, measuring 115 mm. The variations in these parameters offer distinct implications for the behavior and performance of wide beam-column joints.

Hysteresis Curve

The hysteresis curve of a well-performing structure typically exhibits desirable properties such as significant energy dissipation, pinching behavior with narrowing loops, symmetry, ductility, sufficient strength and stiffness, and consistent and predictable behavior.

- Pinching and Symmetry: The hysteresis loops should exhibit pinching behavior, which means that the loops narrow as the loading-unloading cycle progress.
  This pinching behavior indicates stable energy dissipation and implies that the structure can sustain repeated loading cycles without significant degradation in performance. Additionally, the hysteresis loops should be relatively symmetric, indicating that the structure responds similarly during both loading and unloading phases
- Energy Dissipation: The hysteresis curve enclose a relatively large area, indicating significant energy dissipation during cyclic loading. This refers the structure can effectively absorb and dissipate the energy generated by dynamic loads, such as seismic forces, reducing the potential for damage and deformation.

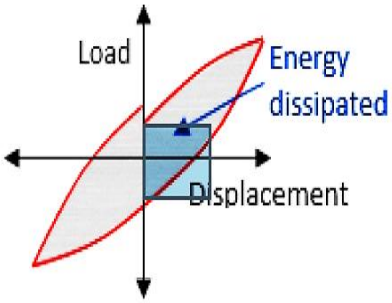

Figure 4- 3 Representation of energy dissipation in hysteresis curve

- Consistency and Predictability: The hysteresis curve should exhibit consistent and repeatable behavior under different loading scenarios. This consistency allows for reliable analysis and prediction of the structure's response to dynamic loads, contributing to the overall safety and performance of the structure.
- Ductility: is crucial in seismic design because it allows the structure to absorb and redistribute energy, thereby enhancing its ability to withstand and recover from seismic forces.

As shown in Figure 4-2, considering the hysteresis curves for different two cases, although the ultimate lateral load has no significant difference as better concrete strength in case14M9 compensate the reduced longitudinal and transverse reinforcement ratio, the hysteresis curve for 16M5 exhibits a comparatively large enclosed area, indicating a significant capacity for energy dissipation. This is attributed to the combination of a high reinforcement ratio with close stirrup spacing enabling the structure to absorb a greater amount of energy before reaching failure. The stirrup yield strength which increases from 400Mpa to 500Mpa also has a positive contribution. Maximum lateral displacement in case 14M9 is 72.746mm but case 16M5 has 74.991mm that showed a 3.086% increase as illustrated in Fig.4-4.

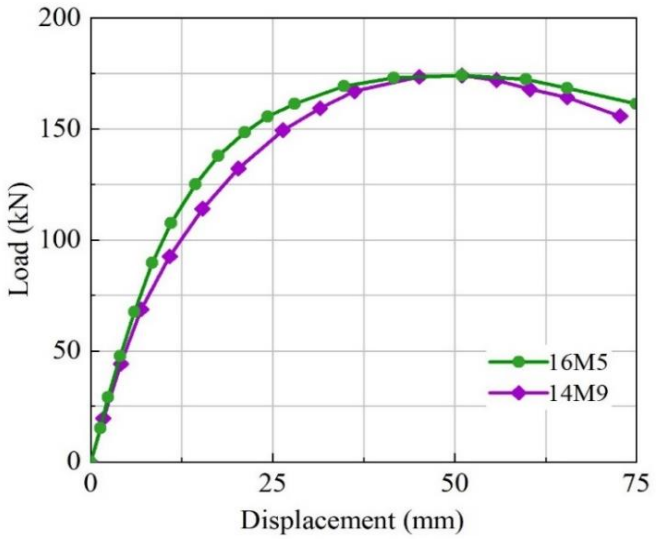

Figure 4- 4 Envelope Curve for 16M5 and 14M9

Ductility

Displacement ductility refers to the ability of a structure or joint to undergo large deformations and absorb energy before failure. Estimating the displacement capacity in wide beam-column connections can be challenging due to the lack of a clear yield point in the load displacement response caused by shear lag. This often requires a particular procedure to determine the yield displacement. In this study, a simplified force displacement response model was used to estimate the yield displacement as presented in Fig.4-5, and the results were found to align well with the measured strain data of the beam bars.[28, 35]

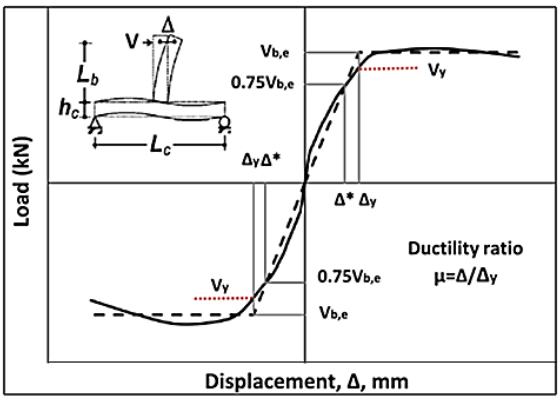

Figure 4- 5 Yield Displacement Determination

Table 4-3 presents the ductility of the specimens, specimen 16M5 observed 8.2% increasing ductility with respect to specimen 14M9. This attributed to confinement contribution from closer spacing of stirrup and increased reinforcement ratio. On the other hand, relative low ductility of specimen 14M9 attributed to low reinforcement ratio and relative brittle behavior of higher-strength concrete, which has higher stiffness and lower strain capacity.

Table 4- 3 Ductility of specimen 14M9 and 16M5

Specimen	Yield Displacement Δy (mm)	Ultimate Displacement Δu (mm)	Ductility (μ)	Comparison
14M9	23.532	72.746	3.091	1.000
16M5	22.411	74.991	3.346	1.082

Failure Mode

The assessment of damage and crack behavior in the specimens primarily focused on evaluating concrete damage under tension and compression as well as analyzing the Von Mises stress experienced by the reinforcement in the RC wide beam-column joint. **Figure 4-6** illustrates the compressive damage of the specimens. As the compressive strength of concrete increases, specimen 14M9 shows a decrease in the amount of damage observed. This suggests that the higher grade of concrete exhibits greater resistance to compressive forces, allowing it to withstand higher loads before reaching its failure point. This increased strength helps minimize the potential for compressive damage, such as crushing or excessive deformation.

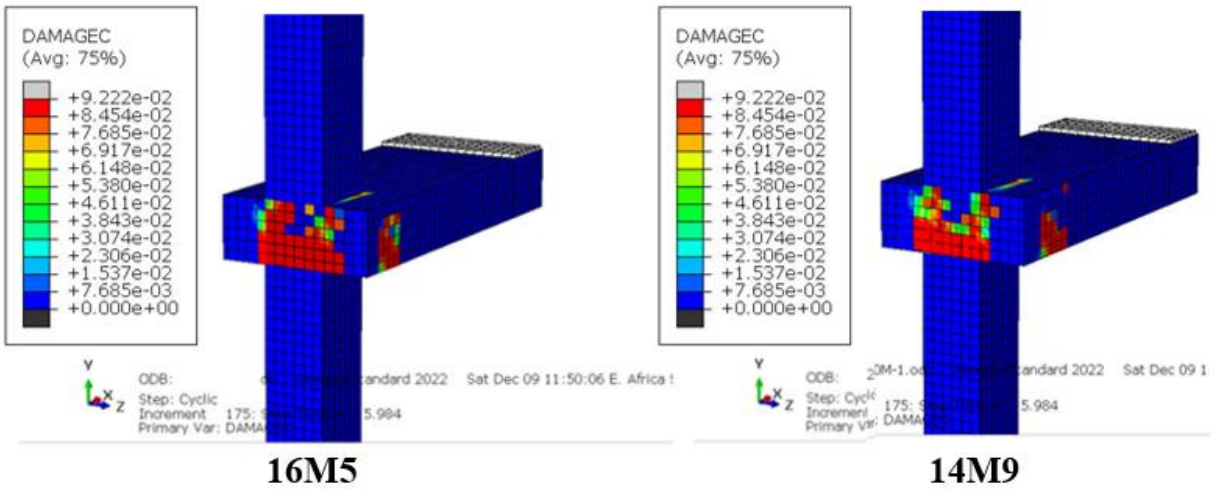

Figure 4- 6 Compressive damage in RC joint specimens

Specimen 14M9 exhibited significant tensile damage despite its higher compressive strength can be shown in Figure 4-7, that can be attributed to its comparatively lower ductility. Despite its ability to withstand compressive loads, Specimen 14M9 proved susceptible to cracking and failure under tensile forces. In contrast, Specimen 16M5, with lower compressive strength, showed lower levels of tensile damage due to its improved ductility resulting from closer spacing and an increased reinforcement ratio.

The reinforcement in Specimen 16M5 provided additional tensile strength, enhancing its resistance to cracking and failure under tensile forces. This result highlight that while higher compressive strength enhances resistance to compressive loads, it does not guarantee improved performance

under tensile forces. The ductility and tensile strength of concrete, influenced by factors like reinforcement spacing and ratio, play a crucial role in mitigating tensile damage.

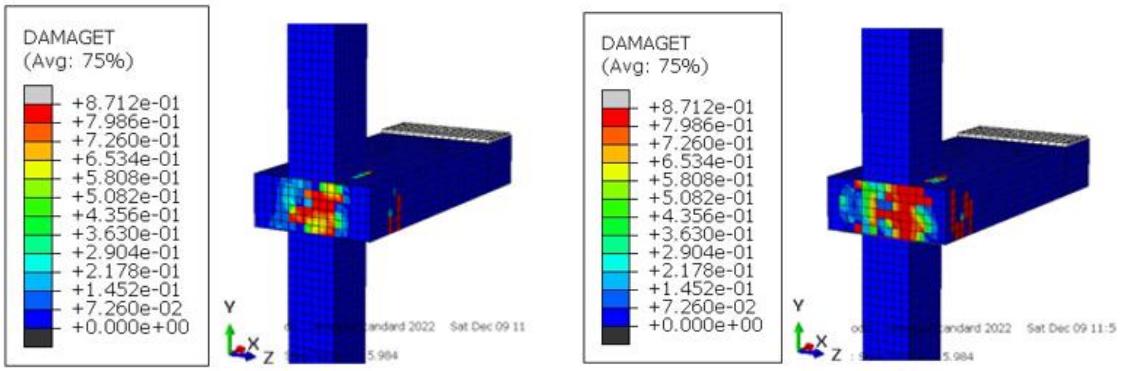

(**16M5**) (**14M9**)

Figure 4- 7 Tensile damage in RC joint specimens

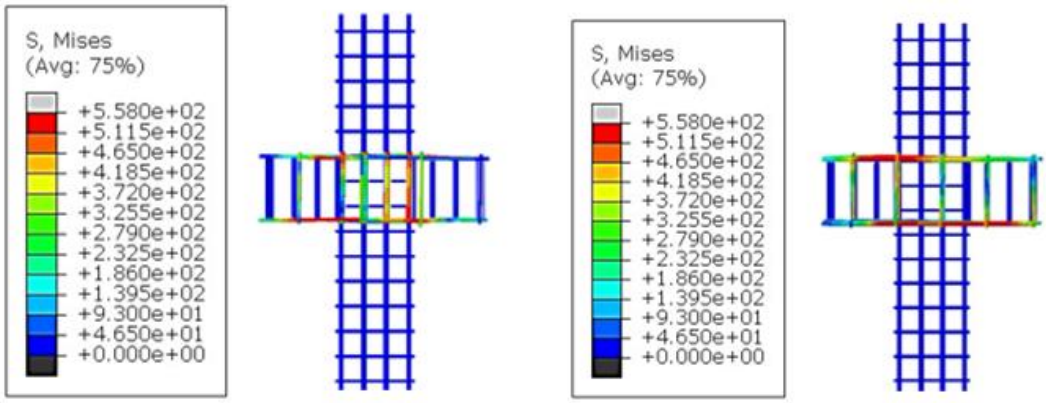

Figure 4- 8 Mises stress in reinforcement of specimens

4.2.2. Effect of diameter of longitudinal bar

The diameter of bar did not significantly influence the load-carrying capacity of the joint but using a greater quantity of smaller diameter bars instead of a smaller quantity of larger diameter offers several advantages in reducing damage in structures. This approach promotes more even load distribution. The figure shows the hysteresis curve of different bar diameters that have a common reinforcement ratio.

Figure in APPENDIX-C show that the diameter of the longitudinal bar had a comparatively noticeable effect on the damage behavior, the use of smaller diameter bars helps to minimize stress concentrations and potential torsional damage.

4.2.3. Effect of transverse beam length

The study aimed to investigate the effect of transverse beam length on the seismic performance of exterior wide beam-column connections. To accomplish this, an additional model, LS4, was examined, where the transverse beam length was increased to three times the length of the validation specimen, resulting in a length of 2250 mm while keeping other parameters unchanged.

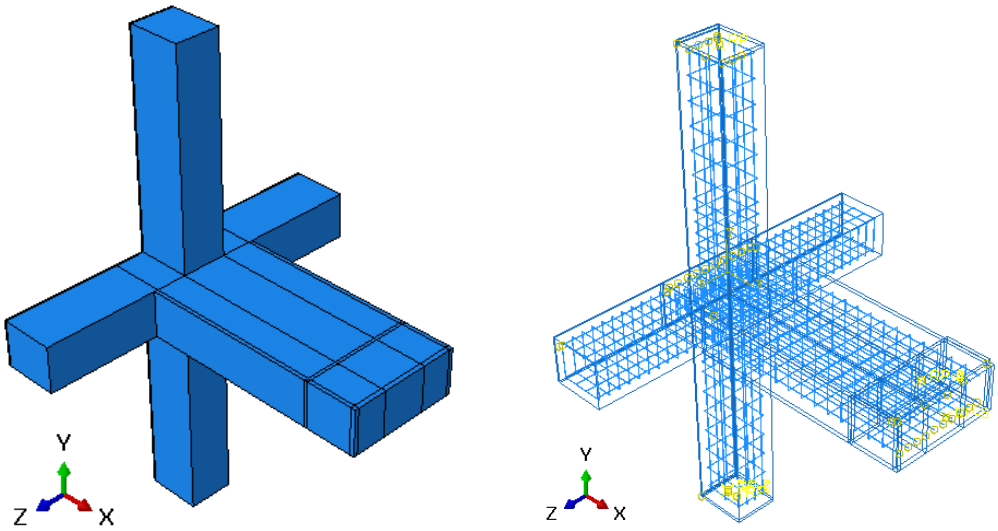

Figure 4- 9 **LS4** Concrete and reinforcement Abaqus model

The comparison of load-displacement envelope curves that presented in Figure 4-10 revealed that specimen LS4 had a very slight reduction in ultimate load capacity. This can be attributed to the small decrease in its torsional capacity of the beam. As the span length increases, the beam experiences greater rotation and torsional deformation under the applied loads. Longer beams typically have lower torsional strength compared to shorter spans due to the increased leverage effect caused by the longer span making it more susceptible to torsional deformations, resulting in decreased shear force transmission and impaired joint shear strength. Consequently, the reduced torsional strength had a minor negative effect on the shear strength of the exterior wide beam-column joint in this particular case.

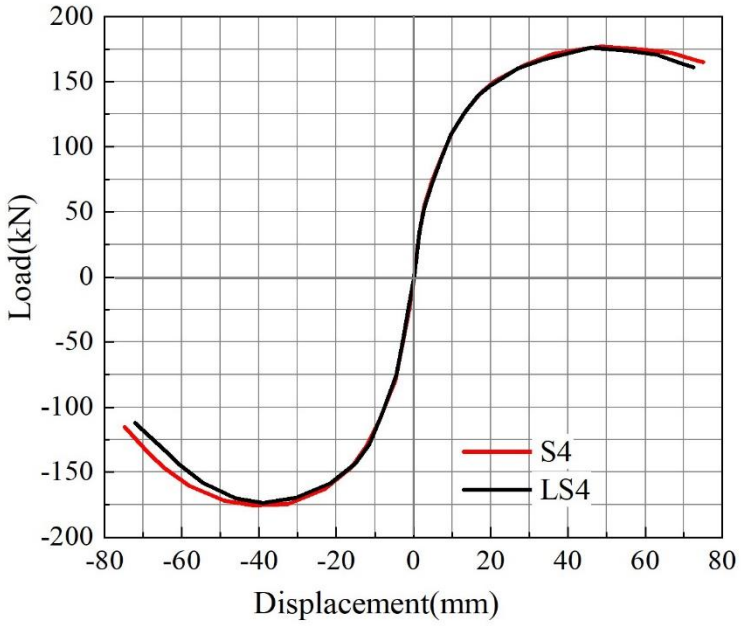

Figure 4- 10 Envelope curve comparison of FE S4 and LS4 model

The experimental setup with a short span of the transverse beam yielded reasonable results and emphasized the significance of analyzing the effective region for shear strength assessment. These findings enhance our understanding of the behavior of wide beam-column joints, enabling more informed design decisions and improved structural performance in practical applications.

5. CONCLUSIONS AND RECOMMENDATIONS

5.1 CONCLUSIONS

Based on the results obtained from the FE analysis, the following observations were obtained:

- The comparison between results of the nonlinear finite element simulation and the experimental data showed that the three-dimensional nonlinear finite element model demonstrates its capacity to predict the shear capacity performance in a reinforced concrete wide beam-column joint that is subjected to both axial and cyclic loading.
- Among the parameters of transverse beam analyzed in this paper, compressive strength of concrete, longitudinal reinforcement ratio, spacing of stirrup and yield strength of stirrup have a significant effect on shear strength of the joint.
- A formula integrating transverse beam parameters has been proposed through regression analysis to enhance the accuracy of shear strength predictions in joints.
- The use of smaller diameter bars throughout the perimeter of the section in the transverse beam led to relatively reduced concrete damage. These results emphasize the significance of considering bar diameter as an important design parameter for ensuring effective control of concrete damage in transverse beams.
- The results of this study suggest that the shear capacity of the RC wide beam-column joint is not significantly influenced by the yield strength of longitudinal bars. Hence, it is valuable to consider other design parameters that directly affect the capacity of the joint.

5.2 RECOMMENDATIONS

- The design of wide-beam-column should incorporate shallow RC transverse beams in the design process of wide beam-column joints.
- Experimental investigation is strongly recommended due to the lack of current studies in this type of joint and its higher level of accuracy in comparison to software simulations
- This study focuses only exterior wide beam-column joint, future research could expand to encompass knee, interior, and corner joints.
- Further research can study additional parameters influencing the joint shear strength. Expanding the parameter range also provides a more comprehensive understanding of structural behavior, enabling performance optimization.

REFERENCES

[1] S. Malviya and M. V. K. Tiwari, "Behaviour of flat slab, waffle slab, ribbed & secondary beam in a multistorey building under seismic response: A review," *Int. J. Res. Appl. Sci. Eng. Technol*, vol. 8, pp. 986-92, 2020.

[2] B. Li and S. A. Kulkarni, "Seismic behavior of reinforced concrete exterior wide beam-column joints," *Journal of structural engineering*, vol. 136, no. 1, pp. 26-36, 2010.

[3] H. Behnam, J. S. Kuang, and K. Abdouka, "Behaviour of RC Spandrel Beam in Exterior Wide Beam-Column Connections," 2016.

[4] H. Behnam, J. Kuang, and R. Y. Huang, "Exterior RC wide beam-column connections: Effect of beam width ratio on seismic behaviour," *Engineering Structures*, vol. 147, pp. 27-44, 2017.

[5] H. Behnam, J. Kuang, H. F. Wong, Q. Huang, and R. Al-Mahaidi, "Analysis of laterally loaded exterior wide beam–column connections," *Magazine of Concrete Research*, vol. 70, no. 10, pp. 500-511, 2018.

[6] A. Committee, "Building code requirements for structural concrete:(ACI 318-02) and commentary (ACI 318R-02)," 2002: American Concrete Institute.

[7] B. Standard, "Eurocode 8: Design of structures for earthquake resistance," *Part*, vol. 1, pp. 1998-1, 2005.

[8] J. M. LaFave and J. K. Wight, "Reinforced concrete wide-beam construction vs. conventional construction: resistance to lateral earthquake loads," *Earthquake Spectra*, vol. 17, no. 3, pp. 479-505, 2001.

[9] H. Behnam and J. Kuang, "Exterior RC wide beam–column connections: effect of spandrel beam on seismic behavior," *Journal of structural engineering*, vol. 144, no. 4, p. 04018013, 2018.

[10] H. Behnam, J. Kuang, and B. Samali, "Parametric finite element analysis of RC wide beam-column connections," *Computers & Structures*, vol. 205, pp. 28-44, 2018.

[11] A. Benavent-Climent, X. Cahís, and J. Vico, "Interior wide beam-column connections in existing RC frames subjected to lateral earthquake loading," *Bulletin of Earthquake Engineering*, vol. 8, pp. 401-420, 2010.

[12] B. Abdelwahed, "A review on reinforced concrete beam column joint: Codes, experimental studies, and modeling," *Journal of Engineering Research (2307-1877)*, vol. 8, no. 4, 2020.

[13] T. Paulay and M. N. Priestley, *Seismic design of reinforced concrete and masonry buildings*. Wiley New York, 1992.

[14] S. S. George and V. Varghese, "General concepts of capacity based design," *Int. J. Innovative Technol. Exploring Eng.(IJITEE),* vol. 1, no. 2, pp. 211-215, 2012.

[15] J. Wang, "Cyclic behaviors of reinforced concrete beam-column joints with debonded reinforcements and beam failure: experiment and analysis," *Bulletin of Earthquake Engineering,* vol. 19, no. 1, pp. 101-133, 2021.

[16] J. L. D. Costa, "Reinforced concrete under large seismic action," *Report BYG. DTUR-076. Danmarks Tekniske Universitet,* 2003.

[17] T. Paulay, R. Park, and M. Preistley, "Reinforced concrete beam-column joints under seismic actions," in *Journal Proceedings*, 1978, vol. 75, no. 11, pp. 585-593.

[18] T. Paulay and A. Scarpas, "The behaviour of exterior beam-column joints," *Bulletin of the New Zealand Society for Earthquake Engineering,* vol. 14, no. 3, pp. 131-144, 1981.

[19] Y. Jemaa, "Seismic behaviour of deficient exterior RC beam-column joints," University of Sheffield, 2013.

[20] W. M. Hassan, *Analytical and experimental assessment of seismic vulnerability of beam-column joints without transverse reinforcement in concrete buildings*. University of California, Berkeley, 2011.

[21] S. Luk and J. Kuang, "Seismic behaviour of RC exterior wide beam-column joints," in *15th World Conference on Earthquake Engineering*, 2012, vol. 14, pp. 10987-10996.

[22] E. Etemadi and T. Vincent, "Mechanical behavior of RC exterior wide beam-column joints under lateral loading: a parametric computational study," *Int. J. Eng. Technol,* vol. 9, pp. 2003-2012, 2017.

[23] M. Rasouli, V. Broujerdian, and A. Kazemnadi, "Predicting the Compressive Stress–Strain Curve of FRP-Confined Concrete Column Considering the Variation of Poisson's Ratio," *International Journal of Civil Engineering,* vol. 18, pp. 1365-1380, 2020.

[24] H. Hatamoto, S. Bessho, and Y. Matsuzaki, "Reinforced concrete wide-beam-to-column subassemblages subjected to lateral load," *Special Publication,* vol. 123, pp. 291-316, 1991.

[25] T. R. Gentry and J. K. Wight, "Wide beam-column connections under earthquake-type loading," *Earthquake Spectra,* vol. 10, no. 4, pp. 675-703, 1994.

[26] J. M. LaFave and J. K. Wight, "Reinforced concrete exterior wide beam-column-slab connections subjected to lateral earthquake loading," *Structural Journal,* vol. 96, no. 4, pp. 577-585, 1999.

[27] E. Yuksel, H. F. Karadogan, I. E. Bal, A. Ilki, A. Bal, and P. Inci, "Seismic behavior of two exterior beam–column connections made of normal-strength concrete developed for precast construction," *Engineering Structures,* vol. 99, pp. 157-172, 2015.

[28] A. Benavent-Climent, X. Cahís, and R. Zahran, "Exterior wide beam–column connections in existing RC frames subjected to lateral earthquake loads," *Engineering Structures,* vol. 31, no. 7, pp. 1414-1424, 2009.

[29] M. Haroon, S. Koo, D. Shin, and C. Kim, "Torsional behavior evaluation of reinforced concrete beams using artificial neural network," *Applied Sciences,* vol. 11, no. 10, p. 4465, 2021.

[30] M. Rashidi and H. Takhtfiroozeh, "The Evaluation of Torsional Strength in Reinforced Concrete Beam," *Mechanics, Materials Science & Engineering Journal,* vol. 7, 2017.

[31] M. S. Ibrahim, E. Gebreyouhannes, A. Muhdin, and A. Gebre, "Effect of concrete cover on the pure torsional behavior of reinforced concrete beams," *Engineering Structures,* vol. 216, p. 110790, 2020.

[32] A. Prabaghar and G. Kumaran, "Theoretical study on the behaviour of rectangular concrete beams reinforced internally with GFRP reinforcements under pure torsion," *International Journal of Civil & Structural Engineering,* vol. 2, no. 2, pp. 579-603, 2011.

[33] A. Gbree, G. Segni, and G. Fikadu, "Assessment of shear strength of interior reinforced concrete beam-column joint," *Zede Journal,* vol. 37, pp. 1-11, 2019.

[34] A. Wosatko, A. Winnicki, M. A. Polak, and J. Pamin, "Role of dilatancy angle in plasticity-based models of concrete," *Archives of Civil and Mechanical Engineering,* vol. 19, pp. 1268-1283, 2019.

[35] H. M. Goldsworthy and K. Abdouka, "Displacement-based assessment of non ductile exterior wide band beam-column connections," *Journal of Earthquake Engineering,* vol. 16, no. 1, pp. 61-82, 2012.

APPENDIX

APPENDIX-A

Envelope curve of the joint specimens for different concrete strength

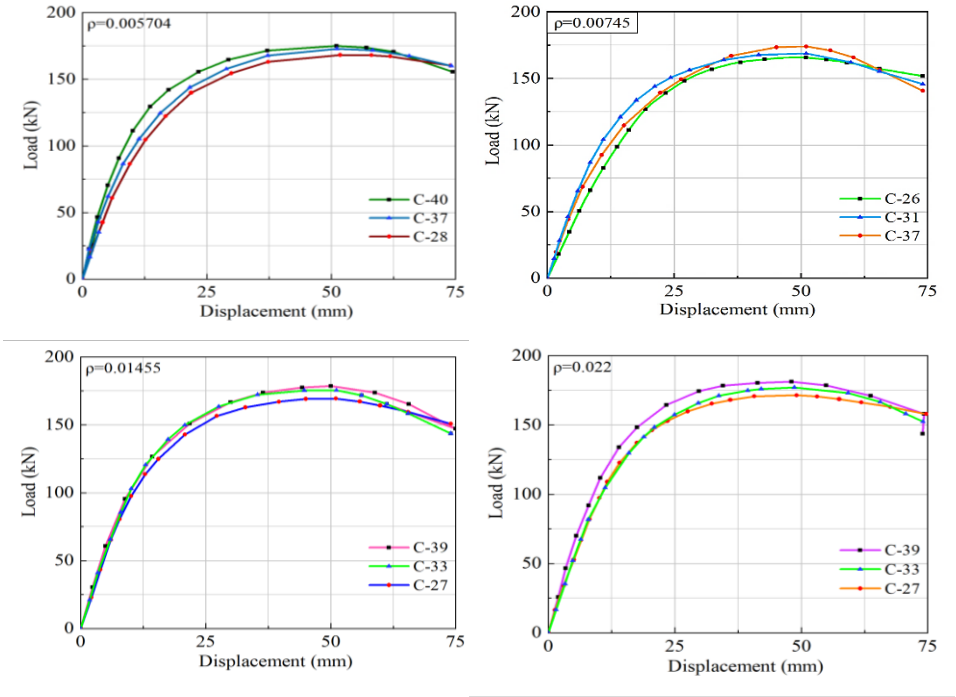

Ultimate lateral load (V_j) of different concrete grade

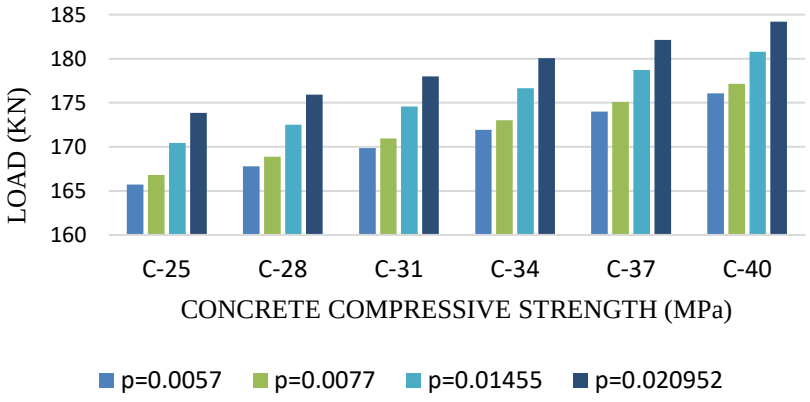

Displacement Ductility Index of Validation Model S4

Specimen	Yield Displacement Δy (mm)	Ultimate Displacement Δu (mm)	Ductility (μ)	Comparison
Experimental	25.00	75.000	3.00	1.000
FEM	24.55	74.991	3.05	1.016

APPENDIX-B

Ductility of the specimens for different concrete grade

ρ	Specimen	Yield Displacement	Ultimate Displacement	Ductility (μ)	Comparison
		Δy (mm)	Δu (mm)		
0.005704	C-28	22.411	74.432	3.321	1.00
	C-37	23.532	74.432	3.163	0.95
	C-40	24.062	74.432	3.093	0.93
0.00745	C-26	24.102	74.442	3.101	1.00
	C-31	24.511	74.442	3.038	0.98
	C-37	26.033	74.442	2.863	0.92
0.01455	C-27	22.103	74.636	3.377	1.00
	C-33	22.341	74.636	3.341	0.99
	C-39	23.344	74.636	3.197	0.95
0.022	C-27	20.004	74.782	3.739	1.00
	C-33	20.468	74.782	3.655	0.98
	C-39	21.445	74.782	3.488	0.93

Ductility of the specimens for different reinforcement ratio

ρ (%)	Concrete Grade	Yield Displacement	Ultimate Displacement	Ductility (μ)	Comparison
		Δy (mm)	*Δu (mm)*		
0.5704	C-39	24.381	74.7816	3.067	1
1.455		23.912	74.7816	3.127	1.011
0.5704	C-26	23.001	74.6362	3.245	1
1.455		22.291	74.6362	3.348	1.032
1.164	C-37	24.104	74.4422	3.088	1
2.2		23.581	74.4422	3.157	1.022
1.164	C-30	22.991	74.4322	3.237	1
2.2		22.311	74.4322	3.336	1.03

Ultimate lateral load (Vj) variation for different stirrup spacing

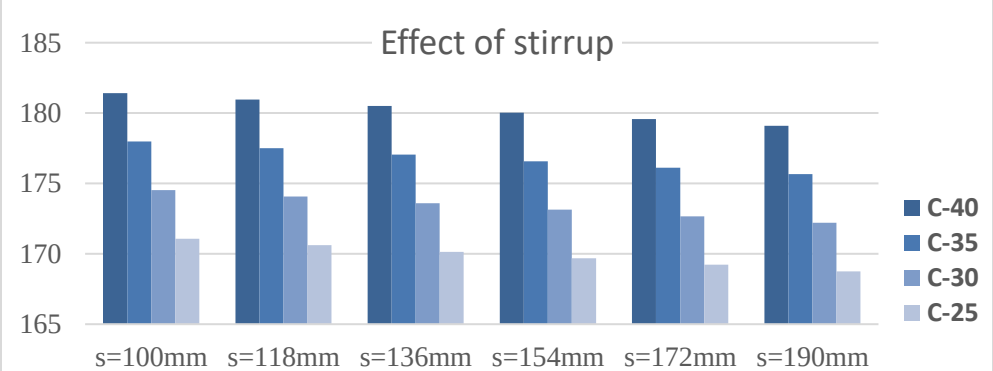

APPENDIX-C

Envelope curve of the joint specimens for different reinforcement ratio

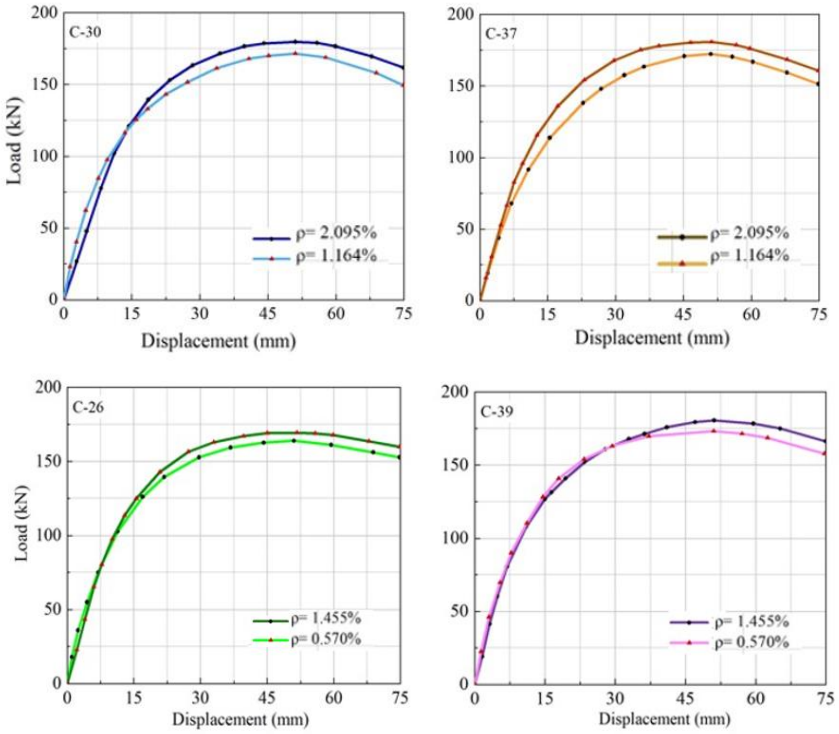

Compressive Damage for different diameter

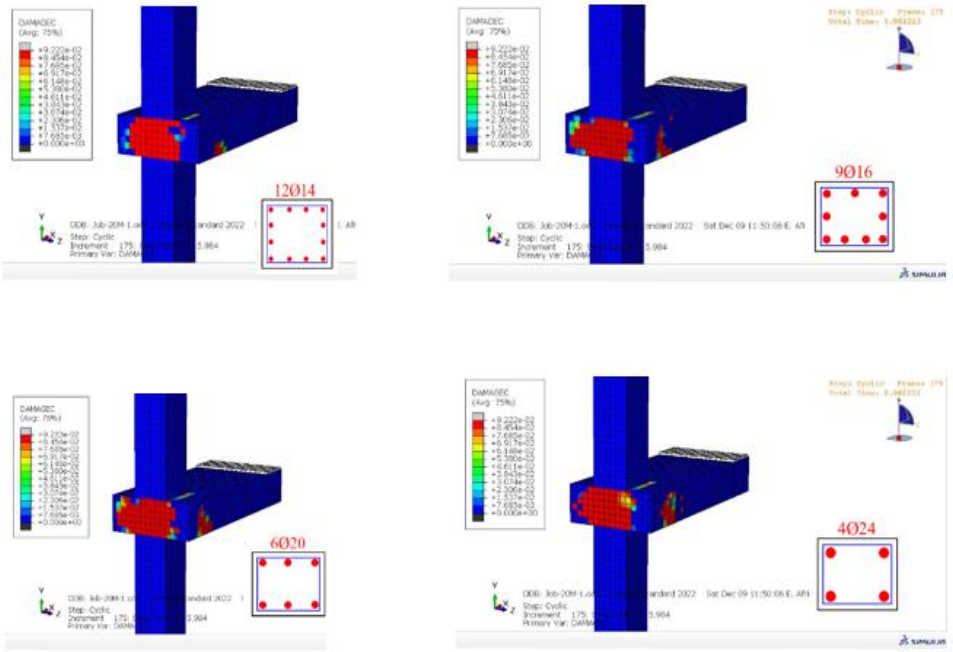

APPENDIX-D

- Compute the balanced steel ratio (ρ_b) using the specified compressive strength of concrete (f'_c) and the yield strength of reinforcement:

$$\rho_b = \frac{f'_c}{f'_c + f_y}$$

- Determine the tension-controlled reinforcement ratio (ρ_t):
- Calculate the maximum tension reinforcement ratio ($\rho_{t,max}$) using the formula:

$\rho_{t,max} = 0.75 * \rho_b$.

- Based on the provided reinforcement ratio (ρ) and $\rho_{t,max}$, determine the tension-controlled reinforcement ratio (ρ_t). If ρ is less than or equal to

$\rho_{t,max}$, then $\rho_t = \rho$

otherwise, $\rho_t = \rho_{t,max}$.

- Calculate the depth of the Whitney stress block (a):

$a = \beta_1 * c$.

Where: β_1 is a coefficient dependent on the strain in the tension reinforcement

c represents the distance from the extreme compression fiber to the neutral axis.

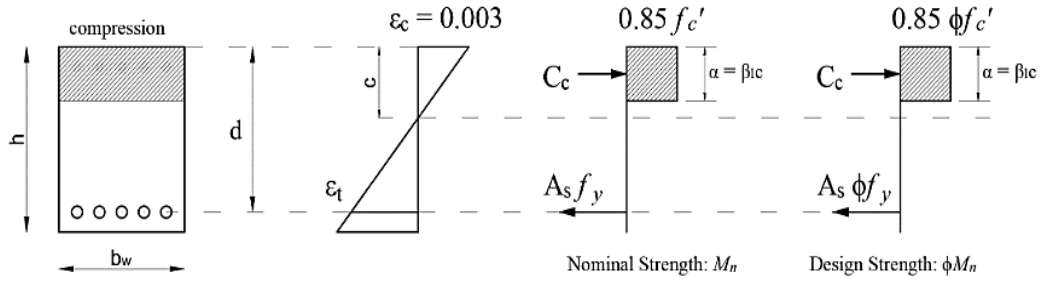

- Calculate the nominal flexural strength ($M_{n,b}$):

$$M_{nb} = \phi A_s f_y (d - a/2)$$